Mechanistic evaluation of a novel cyclohexanone derivative's functionality against nociception and inflammation: an *in-vitro*, *in-vivo* and *in-silico* approach.

8 **Jawad Khan[1], Gowhar Ali[*1], Umer Rashid[2], Rasool Khan[3], Muhammad Saeed Jan[4], Rahim**

9 **Ullah[1], Sajjad Ahmad[5], Sumra Wajid Abbasi[6], Atif Ali Khan Khalil[6], Robert D. E. Sewell[7]**

12 [1]Department of Pharmacy, University of Peshawar, Peshawar 25120, Pakistan

13 [2]Department of Chemistry, COMSATS University Islamabad, Abbottabad Campus, Pakistan

14 [3]Institute of Chemical Sciences, University of Peshawar, Pakistan 25120, Pakistan

15 [4]Department of Pharmacy, Faculty of Biological Sciences, University of Malakand, Chakdara
16 18000 Dir (L), Pakistan

17 [5]Department of Health and Biological Sciences, Abasyn University, Peshawar 25000, Pakistan
18 [6]Department of Biological Sciences, National University of Medical Sciences, Rawalpindi,
19 46000, Pakistan
20 [7]School of Pharmacy and Pharmaceutical Sciences, Cardiff University, Cardiff CF10 3NB. UK

25 *** Corresponding author:**

26 **Dr. Gowhar Ali,**
27 **(B.Sc., Pharm.D., Ph.D.)**
28 **Assistant Professor**
29 Department of Pharmacy
30 University of Peshawar,
31 Peshawar-25120, KP, PAKISTAN.
32 Cell # 00923339317832
33 Contact: Tel: *+92 091 9216750;*
34 Fax:+92-91-9218131
35 **ORCID**:: https://orcid.org/0000-0002-9749-0645

37
38

Highlights

39

40

41 -A synthesised anti-inflammatory cyclohexanone (CHD) was tested *in vivo* and *in vitro*

42 -CHD inhibited COX-2 and 5-LOX enzymes plus COX-2, TNF-α and IL-1β mRNA expression

43 -CHD also produced GABA$_A$ and opioid mediated inhibitory activity in nociceptive tests

44 -In silico CHD had preferential affinity for GABA$_A$, opioid and COX-2 target sites

45 -CHD may possess therapeutic effectiveness in the management of inflammation and pain

46

47 **Graphic Abstract**

48

49

50

51
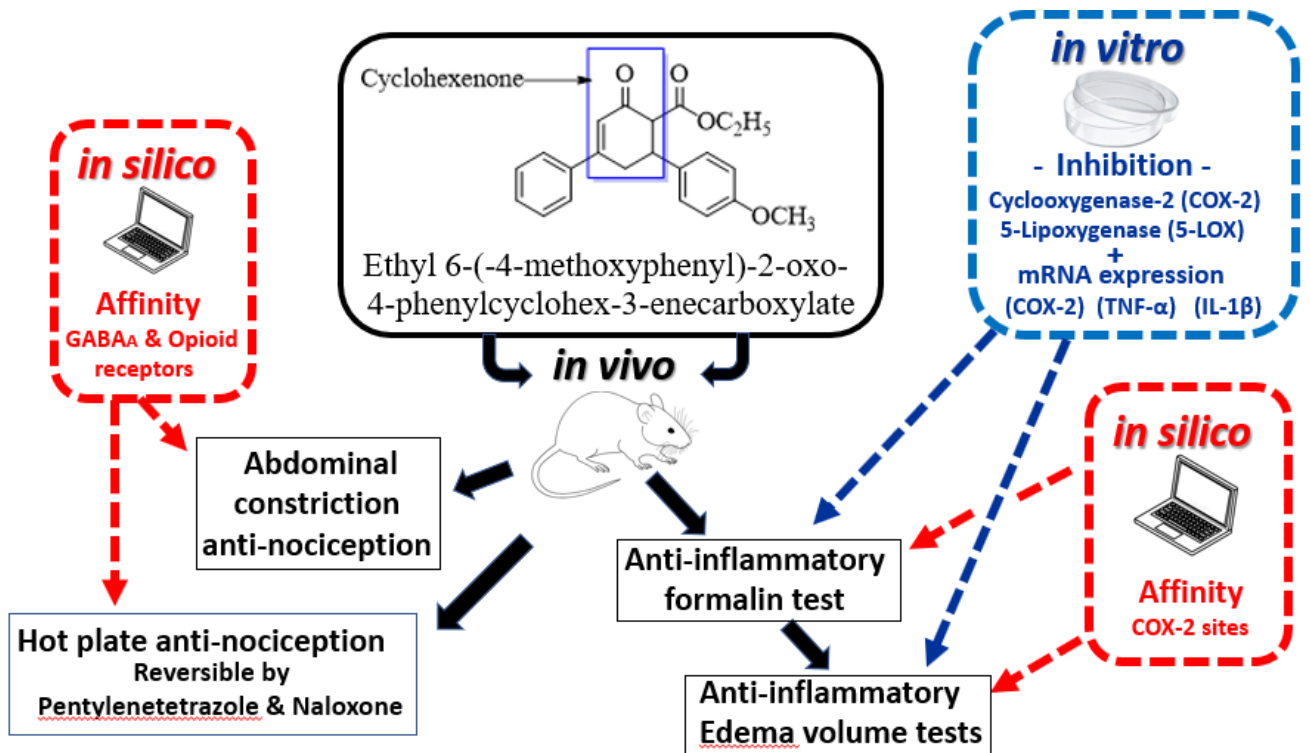
Abstract

The synthesis of a novel cyclohexanone derivative (CHD; Ethyl 6-(4-metohxyphenyl)-2-oxo-4-phenylcyclohexe-3-enecarboxylate) was described and the subsequent aim was to perform an *in vitro*, *in vivo* and *in silico* pharmacological evaluation as a putative anti-nociceptive and anti-inflammatory agent in mice. Initial *in vitro* studies revealed that CHD inhibited both cyclooxygenase-2 (COX-2) and 5-lipoxygenase (5-LOX) enzymes and it also reduced mRNA expression of COX-2 and the pro-inflammatory cytokines TNF-α and IL-1β. It was then shown that CHD dose dependently inhibited chemically induced tonic nociception in the abdominal constriction assay and also phasic thermal nociception (i.e. anti-nociception) in the hot plate and tail immersion tests in comparison with aspirin and tramadol respectively. The thermal test outcomes indicated a possible moderate centrally mediated anti-nociception which, in the case of the hot plate test, was pentylenetetrazole (PTZ) and naloxone reversible, implicating GABAergic and opioidergic mechanisms. CHD was also effective against both the neurogenic and inflammatory mediator phases induced in the formalin test and it also disclosed anti-inflammatory activity against the phlogistic agents, carrageenan, serotonin, histamine and xylene compared with standard drugs in edema volume tests. *In silico* studies indicated that CHD possessed preferential affinity for GABA$_A$, opioid and COX-2 target sites and this was supported by molecular dynamic simulations where computation of free energy of binding also favored the formation of stable complexes with these sites. These findings suggest that CHD has prospective anti-nociceptive and anti-inflammatory properties, probably mediated through GABAergic and opioidergic interactions supplemented by COX-2 and 5-LOX enzyme inhibition in addition to reducing pro-inflammatory cytokine expression. CHD may therefore possess potentially beneficial therapeutic effectiveness in the management of inflammation and pain.

3

81

1. Introduction

The process of drug discovery and development incorporating a novel chemical moiety with a desirable therapeutic profile is a challenging task nowadays (DiMasi et al., 2010). Extensive research has been carried out on pain and inflammation over a number of years, particularly because these pathological conditions can greatly influence patient quality of life (Ali et al., 2015; Chapman and Gavrin, 1999; Shahid et al., 2017a; Shahid et al., 2017b). Pathologically, pain may be categorized as nociceptive, neuropathic or inflammatory and if protracted, it may progress into a chronic pain syndrome involving additional symptoms such as anxiety and depression. Nociceptive pain is typically initiated by stimulation of somatic sensory receptors designated as nociceptors, which then transmit pain impulses to the central nervous system (CNS). Alternatively, neuropathic pain arises from damage or lesions to the nervous system (Van Hecke et al., 2014). Active inflammation is the hallmark of inflammatory pain and is characterized by the presence of inflammatory mediators such as interleukin, TNF-α, prostaglandins (PGE2, PGI2, TXA2), histamine, serotonin, bradykinin and leukotrienes (LTs) (Fernandes et al., 2015). These biochemical substances produce changes in neuronal sensitivity and invoke the onset of tissue hypersensitivity associated with inflammation (Kidd and Urban, 2001). Currently, opioids and non-steroidal anti-inflammatory drugs (NSAIDs) are the analgesic agents of choice often utilized in the management of inflammatory pain. However, it is well documented that persistent use of NSAIDs may well cause deleterious effects such as ulceration, hemorrhage or even perforation in the gastrointestinal tract, cardiovascular system disorders and kidney damage (Gutthann et al., 1996; Jones et al., 2008). Similarly, opioid analgesics are considered highly effective as analgesics, but they are associated with dependence liability and other side effects which may limit their

104 usefulness (Laxmaiah Manchikanti et al., 2010; Mayer et al., 1995; Shahid et al., 2016).

105 Consequently, there is a genuine need for substitute drugs that retain the analgesic and anti-

106 inflammatory effectiveness of conventional analgesic agents without their untoward effects

107 (Fawad et al., 2018; Islam et al., 2017; Islam et al., 2019).

108 The key role of the cyclohexenone ring is well established in the field of biomedical research. It

109 has been documented that this functionality is an integral part of several interesting compounds

110 and is of considerable significance for the development of potentially valuable drugs (Das and

111 Manna, 2015; Fang et al., 2012). Chemically, the cyclohexenone nucleus, serves as a convenient

112 intermediate for synthesizing various heterocyclic compounds including fused pyrazoles,

113 isoxazoles, quinazolines (Senguttuvan and Nagarajan, 2010) and 2H-indazole (Gopalakrishnan et

114 al., 2008). Cyclohexenones are cyclohexane derivatives with a carbonyl group at position-1 and a

115 carbon-carbon double bond at position-2 (Fig. 1). The enone functional group and substitution at

116 a carbon atom in the six membered ring have been used to synthesize other substituted

117 cyclohexenones (Johnson et al., 2016). The pharmacological properties of cyclohexenone

118 derivatives include anti-inflammatory and anti-nociceptive effects (Ahmadi et al., 2012; Lednicer

119 et al., 1981a; Lednicer et al., 1981b; Liu et al., 2013; Ming-Tatt et al., 2013; Ming-Tatt et al., 2012;

120 Sheorey et al., 2016; Wang et al., 2011) as well as anti-neuropathic and antioxidant activity (Khan

121 et al., 2019). The present study was undertaken to evaluate a novel cyclohexenone derivative

122 (CHD; Ethyl 6-(4-metohxyphenyl)-2-oxo-4-phenylcyclohexe-3-enecarboxylate) as a possible

123 inhibitor of cyclooxygenase-2 (COX-2) and 5-LOX pro-inflammatory enzymes and subsequently

124 examine its effects against nociception using *in vivo* mouse models of pain and inflammation.

125 Additionally, the anti-nociceptive activity of CHD was also investigated in the presence of

126   pentylenetetrazole (PTZ) and naloxone in order to probe any possible underlying mechanisms,

127   which might have been corroborated by *in silico* and *in vitro* studies.

128

129   **2. Material and methods**

130   2.1. *Chemicals and drugs*

131   Naloxone, serotonin, histamine, PTZ, xylene, indomethacin, lambda carrageenan and aspirin were

132   purchased from (Sigma-Aldrich, USA). Formaldehyde was procured from Merck (Germany),

133   glacial acetic acid was obtained from Pancreac (Spain), tramadol (Tramal® 50mg/ml) was

134   acquired from Searle Ltd (Pakistan). Fresh preparation of chalcone was carried out in the

135   laboratory of ICS (University of Peshawar, Pakistan). Ethyl acetoacetate, ethyl acetate and

136   potassium carbonate were purchased from Merck (Pakistan). N-hexane and ethanol were procured

137   from Scharlau (Lahore, Pakistan). The cDNA synthesis kit, TRIzol reagent, master mix and

138   primers were acquired from Thermofishcer Scientific (USA).

139   *2.2. Chemistry*

140   *2.2.1. General*

141   A Gallenkamp melting point apparatus was used to determine melting points. Purity was checked

142   by thin layer chromatography (TLC). A Shimadzu IR Prestige-21 FT-IR Spectrometer Instrument

143   (Tokyo, Japan) was utilized to record the Infrared spectra. ^{13}C and ^{1}H NMR analyses (Agilent AV-

144   300,400 and 500 Tokyo, Japan) were accomplished with D_2O and DMSO-d_6 as solvents. Mass

145   spectra (ESI-MS) were obtained on (Qp 2010 plus, Shimadzu, Tokyo, Japan). Perkin Elmer 2400

146   CHN/O Analyzer was operated to determine Elemental analysis.

147

148 *2.2.2. Synthesis of Ethyl 6-(4-metohxyphenyl)-2-oxo-4-phenylcyclohexe-3-enecarboxylate*

149 The synthesis was conducted according to the synthetic protocol as shown in Scheme 1. (E)-3-(-

150 4-methoxyphenyl)-1-phenylprop-2-en-1-one (10 mmol) was refluxed with ethyl acetoacetate (20

151 mmol) in the presence of K_2CO_3 catalyst in 20 ml of ethanol for 3 hr. The product obtained was

152 recrystallized from ethanol; a brownish yellow powder was obtained having a yield of 85 %. M.p

153 = 92-95 ^{0}C; Rf = 0.51 *n*-Hexane/ethyl acetate (7:3); IR (KBr) υmax cm-1: 3077 (Ar-H), 1689

154 (ketone C=O), 1735 (Ester C=O) 2870 (Aliphatic C-H); ^{1}H-NMR (CDCl$_3$, 400MHz) δ:6.9-7.5 (m,

155 Ar-H),3.05 (d, 2H, J= 2.3), 2.9 (t,1H J=5.0, C-3), 2.6-2.8(q, 5H, CH_2CH_3, J=7.0); ^{13}C-NMR (100

156 MHz, CDCl$_3$) δ: 199.0 (C=O), 125-130 (Ar-CH), 112 (C-6), 40.2 (OCH$_3$), 159.0 (C-19), and 44.39

157 (C-3). EI-MS; m/z (rel. int. %) 351 (M+), CHN Anal. Calcd for: C, 75.41; H, 6.33; O, 18.26.

158 Found: C, 74.81; H, 6.38. Formula: $C_{22}H_{22}O_4$, C=22, H=22, and O=4.

159
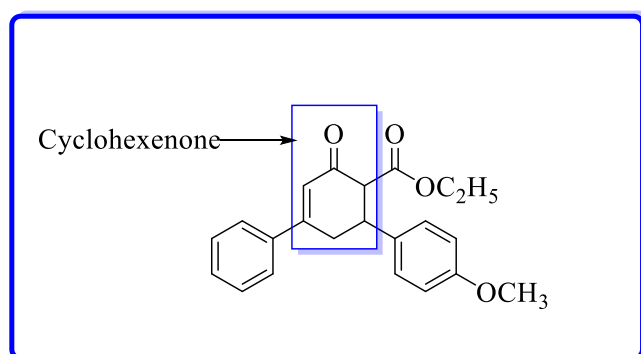
160 **Fig. 1.** Chemical structure of Ethyl 6-(-4-methoxyphenyl)-2-oxo-4-phenylcyclohex-3-

161 enecarboxylate

162

163

164
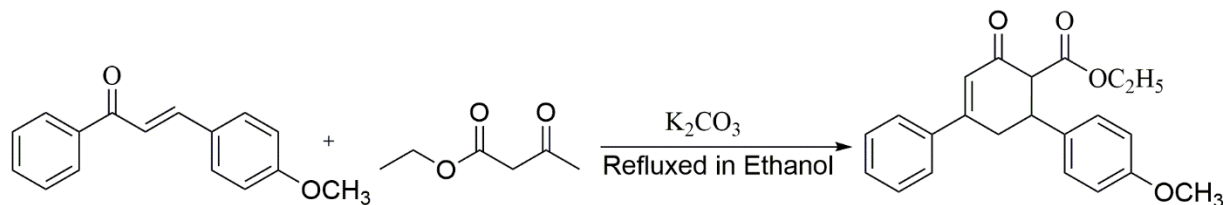
Scheme 1. Synthetic scheme of Ethyl 6-(4-metohxyphenyl)-2-oxo-4-phenylcyclohexe-3-enecarboxylate

2.3. In vitro activities

2.3.1. 5-LOX inhibition assay

The inhibitory potential of CHD was examined by utilizing human recombinant 5-LOX. In this assessment, the enzyme inhibition was determined through residual enzyme potential following 10 to 15 min incubation at 25 ℃ in an incubator (Jan et al., 2020; Wisastra et al., 2013). The activity was estimated through linoleic acid (lipoxygenase substrate) conversion into hydroperoxy-octadecadienoate (HPOD). The alteration rate was calculated in the form of absorbance at 234 nm with UV- visible spectrophotometer. Ethylene diamine tetra acetic acid (EDTA 2 mM) and $CaCl_2$ (2 mM) containing Tris buffer (50 mM) of PH 7.5 was used as an assay buffer for this assay. The enzyme 5-LOX (20,000 U/ml) was diluted with buffer in a ratio of 1:4000. The assay buffer was then diluted with 100 mM of inhibitor formerly blended with DMSO. Linoleic acid was then diluted with ethyl alcohol to 20 mM. Subsequently, various concentrations of CHD ranging from 31.25 to 1000 µg/ml and 1 ml of enzyme solution (1:4000) was mixed with 100 µl adenosine triphosphate (2 mM), 790 µl of Tris buffer plus 100 µl inhibitor (1mM) and then incubated for ten min duration. Then to this mixture was added 10 µl of substrate solution (20mM) and after ten seconds mixing of the enzyme with substrate, the substrate conversion rate was monitored. The

184 reaction rate in the absence of inhibitor was employed as positive control. The standard inhibitor

185 agent used in this assay was zileuton.

186 *2.3.2. COX-2 Inhibition assay*

187 The COX-2 inhibitory activity of the test compound was evaluated according to a previously

188 validated procedure (Burnett et al., 2007; Jan et al., 2020). A COX-2 enzyme solution (300 U/ml)

189 was prepared. For activation, 10 µl of enzyme solution was kept for 5 to 6 min on ice (4 $^{\circ}$C) and

190 then mixed with 50 µl of co-factor solution comprising 0.9 mM glutathione, 1 mM hematin in 0.1

191 mM Tris buffer (pH 8.0) and 0.24 mM tetramethyl-p-phenylenediaminedihydrochloride (TMPD).

192 Then various concentrations (31.25 to 1000 µg/ml) of test sample (20 µl) plus enzyme solution

193 (60 µl) were maintained at room temperature for 5 to 10 min, followed by initiation of the reaction

194 by adding 30 mM arachidonic acid (20 µl) and keeping this mixture at 37 $^{\circ}$C for a duration of 15

195 min. Afterwards, the reaction was terminated by addition of hydrochloric acid (HCL) and

196 absorbance was measured via a UV-visible spectrophotometer at 570 nm. COX-2 percentage

197 inhibition was calculated from the absorbance value per unit time. In the study Celecoxib was

198 utilized as the standard inhibitor agent.

199 *2.3.3. Reverse transcription polymerase chain reaction (RT-PCR)*

200 Post-mortem mouse paw sub plantar tissues were removed 5 h after carrageenan administration

201 and RNA was extracted using TRIzol reagent according to the manufacturer's protocol. The total

202 RNA was reverse transcribed to cDNA following a standard protocol. The primers for targeted

203 genes use were;

204 **COX-2**: F-5'-GGAGAGACTATCAAGATAGTGATC -3', R- 5'- ATGGTCAGTAGA-CTTT-

205 TACAGCTC-3'.   **TNF-α:**   F-5'-CTTCTCCTTCCTGATCGTGG-3';   R-5'-GCTGGTTAT-

206 CTCTCAGCTCCA-3'. **IL-1β**: F-5'-AGAAGCTTCCACCAATACTC-3', R-5'-AGCACCTAG-

207 TTGTAAGGAAG-3'. **GAPDH**: F-5'-TGCACCACCAACTGCTTAGC-3'; R- 5'-GGCATG-

208 GACTGTGGTCATGAG3' was used as a housekeeping gene (Cheon et al., 2009; Khalid et al.,

209 2018). Amplified products were separated using 1.5% Agarose gel electrophoresis, analyzed with

210 image J software (Almeer et al., 2019; Ullah et al., 2021).

211 *2.4. In vivo pharmacological evaluation*

212 *2.4.1. Animals*

213 Mice (Balb-C) of either sex weighing 18-30 g were used during the investigation unless otherwise

214 stated. Animals were maintained on standard laboratory food and water *ad libitum* at an ambient

215 temperature of $22 \pm 2^{\circ}C$ through a thermostatically controlled air conditioning system on a 12/12

216 h light and dark cycle and they were habituated to laboratory conditions for two h before

217 experiments.

218 *2.4.2. Ethical approval*

219 The study and all *in vivo* protocols were conducted under a project entitled "Studies on the

220 nociceptive, inflammatory and neuropathic pain relieving potential of a cyclohexenone

221 derivative." It was approved by the Research Ethical Committee of the Department of Pharmacy,

222 University of Peshawar, Pakistan which issued a certificate number of 01/EC/18/Pharm.

223 Furthermore, animal experiments were performed in compliance with the Animals Scientific

224 Procedure Act UK (1986).

225

226

227

228 *2.4.3. Acute toxicity study of compound CHD*

229 The acute toxicity profile of CHD was evaluated after intraperitoneal (i.p) injection of selected

230 doses (on a sequential dose-doubling increasing scale viz 15, 30, 60, 120 or 240 mg/kg (n=6)).

231 Animals were observed at 30-60 min and 24-72 h for any abnormal behaviour (Akbar et al., 2016).

232 *2.4.4. Anti-nociceptive activity*

233 *2.4.4.1. Anti-nociceptive activity of compound CHD and a standard drug in the acetic acid*

234 *abdominal constriction test*

235 Food and water were withdrawn 120 min prior to animal experiments. One percent acetic acid (10

236 ml/kg) i.p injection was used to induce abdominal constriction as a reflection of tonic nociception.

237 Five min after acetic acid i.p injection, the incidence of abdominal constrictions was recorded over

238 a 20 min period (Abbas et al., 2011). The animals were randomly allocated to different

239 investigational groups (n=6). Group I received normal saline as vehicle, group II-IV received

240 standard aspirin (15-45 mg/kg), group V-VII received test compound (CHD) (15-45 mg/kg) via

241 i.p injection, 30 min prior to 1% acetic acid injection. Percentage analgesia was calculated using

242 the following formula:

243 % protection = (1- mean number of abdominal constrictions of the treated drug / mean number

244 of abdominal constrictions of the vehicle control) × 100

245 *2.4.4.2. Anti-nociceptive activity of compound CHD compared to a standard drug in the hot plate*

246 *test*

247 The hot plate analgesiometer, was kept at a constant temperature of 54 ± 0.1^0 C. After placement on

248 the plate, animal nociceptive reaction latencies (s) were determined to the following escape end

249 points: paw licking, flinching or jumping and a 30 s cut off time was imposed after which mice

250   were removed from the stimulus (Ahmad et al., 2017; Rukh et al., 2020). Animals were randomly

251   assigned to groups (n=6) and administered saline or drug treatment intraperitoneally. Group I

252   received normal saline as vehicle, group II received standard drug (tramadol, 30 mg/kg, i.p),

253   groups III-V received the trial compound (CHD, 15-45 mg/kg, i.p).

254   *2.4.4.3. Pharmacological antagonism study of CHD compared to a standard drug*

255   In order to evaluate the possible involvement of $GABA_A$ or opioid receptors in the anti-nociceptive

256   activity of CHD, mice were administered PTZ (15 mg/kg; i.p) or naloxone (1 mg/kg;

257   subcutaneously (s.c)) 10-20 min prior to i.p dosing with saline, CHD or standard drug. Hot plate

258   latencies were recorded 30,60 and 90 min after administration of each drug (Muhammad et al.,

259   2012). Percentage protection against nociception was determined using the following formula:

260   % protection = (Test latency−baseline latency)/ (cut off time−baseline latency) × 100

261   *2.4.4.4. Anti-nociceptive activity of CHD compared to a standard drug in the tail immersion test*

262   Each animal was gently held in a vertical position and half of the tail was immersed in a water

263   bath maintained at a temperature of 55±0.5 °C. A nociceptive reaction latency (s) was determined

264   to a tail flick end point and a cut off time of 15 s imposed after which animals were removed from

265   the stimulus. Any non-responders within the cut-off time were excluded from the study. The

266   vehicle, standard tramadol (30 mg/kg) and test compound (15-45 mg/kg) were administered i.p to

267   their respective groups. The readings were taken at 30, 60, 90 and 120 min after drug

268   administration (Sewell and Spencer, 1976).

269

270

271 *2.4.4.5. Anti-nociceptive activity of CHD and standard drug in the formalin induced biphasic pain*

272 *model*

273 Mice were administered a sub plantar injection of 20µl of freshly prepared 2 % formalin in the

274 right hind paw. Thirty min prior to formalin injection, groups I-VI, received intraperitoneally

275 normal saline as vehicle, standard drugs indomethacin (10 mg/kg) or diclofenac (10 mg/kg), and

276 CHD (15-45mg/kg). The nociceptive reaction time (s) (latency to biting, licking, paw lifting or

277 flinching) was measured in two phases: first phase (0 to 5 min) and second phase (10-30 min) after

278 the formalin injection (Silva et al., 2017; Maione et al., 2020).

279 *2.4.5. Anti-inflammatory activity*

280 *2.4.5.1. Anti-inflammatory activity of compound CHD and standard in a carrageenan induced paw*

281 *edema model*

282 Mice were treated with normal saline, aspirin (50-150 mg/kg) or test compound (CHD, 15-45

283 mg/kg, i.p) 30 min before s.c injection of 0.05 ml of freshly constituted carrageenan (1 %) in the

284 right hind paw. A digital Plethysmometer was utilized to determine the inflammation in terms of

285 paw edema volume (ml) at hourly intervals up to 5 h post carrageenan injection (Ali et al., 2013).

286 *2.4.5.2. Anti-inflammatory activity of compound CHD and standard drug in a histamine induced*

287 *paw edema model*

288 Inflammation was induced in mice (25-30 g) by sub plantar injection of 0.1 ml freshly constituted

289 histamine (1 mg/ml) in the right hind paw. Paw inflammation swelling was measured by means of

290 plethysmometer previously described in the carrageenan test (Mequanint et al., 2011).

291

292 *2.4.5.3. Anti-edema activity of CHD and a standard drug in the serotonin induced paw volume*

293 *model*

294 Mice were administered serotonin (0.001 mg/ml s.c) into the plantar surface of the right hind paw.

295 The ensuing inflammation and paw edema was measured by plethysmometer (Masresha et al.,

296 2012).

297 *2.4.5.4. Anti-inflammatory action of compound CHD and standard drug in the xylene provoked*

298 *ear edema model*

299 In mice weighing 25-35 g, ear edema was evoked by topical application of 0.03 ml of xylene to

300 the internal and outer surface of the right ear while the left ear was used as control. Thirty min

301 before induction of xylene edema, saline vehicle was administered i.p to group I, standard

302 indomethacin (10 mg/kg) or diclofenac (15 mg/kg) to groups II-III and test compound CHD (15-

303 45 mg/kg) to groups IV-VI respectively. Subsequently, 15 min after xylene application, animals

304 were killed and the ears were amputated then weighed. The mean weight difference between right

305 and left ears was then determined (Manouze et al., 2017).

306

307

308

309 *2.5. In silico activity*

310 *2.5.1. Docking studies*

311 Docking studies were executed through the Molecular Operating Environment (MOE) version

312 2016.08 docking program. Three-dimensional (3D) structures of the enzymes, $GABA_A$ and opioid

313 receptors with their co-crystalized ligands were obtained from the Protein Data Bank as listed in

314 Table 1. The docking algorithm was validated by re-docking of native ligands as shown in Table

315 1. The computed root mean square deviation (RMSD) between the experimental and re-docked

316 poses was found within a threshold limit < 2 Å. The 3D structures of the compound were

317 constructed in MOE by utilizing Builder Module. Energy minimization of the ligand, preparation

318 of structures of the downloaded enzymes and active site identification was carried out according

319 to our earlier validated methods (Iftikhar et al., 2017; Iftikhar et al., 2018; Rashid et al., 2016).

320 Assessment of docking outcomes and scrutiny of their surface with graphical demonstrations were

321 accomplished with discovery studio visualizer and MOE (Systemes, 2015).

322

323 **Table 1**
324 Protein Data Bank (PDB) code numbers, names of their co-crystalized ligands and resolution for
325 the enzymes studied.
326

Enzyme/Receptor	PDB code	Co-crystalized ligand	Resolution (Å)
COX-1 enzyme	1EQG	Ibuprofen	2.61
COX-2 enzyme	1CX2	1-Phenylsulfonamide-3-trifluoromethyl-5-parabromophenylpyrazole (SC-558)	3.00
GABA$_A$ receptor	4COF	Benzamidine	2.97
μ-opioid receptor	4DKL	β-Funaltrexamine (μ-opioid receptor antagonist)	2.8
δ-opioid receptor	4EJ4	Naltrindole (δ-opioid receptor antagonist)	3.4
κ-opioid receptor	4DJH	(3R)-7-Hydroxy-N-{(2S)-1-[(3R,4R)-4-(3-hydroxyphenyl)-3,4-dimethylpiperidin-1-yl]-3-methylbutan-2-yc-1,2,3,4-tetrahydroisoquinoline-3-carboxamide (JDC)	2.9

327
328

329

2.5.2. Molecular Dynamic Simulation of Complexes

331 Molecular Dynamic (MD) simulations were performed using the same protocol as explained in

332 our previous study (Abbasi et al., 2016). MD simulations facilitate understanding of the binding

333 pattern and determine the stability of selected receptor-CHD docked complexes. Using AMBER

334 18 software, six different systems were prepared to run MD simulations for 50 ns each (Case et

335 al., 2010). In order to verify the structural variations and convergence of the simulated systems,

336 the CPPTRAJ module of AmberTools18's was used to estimate the RMSDs for all the studied

337 systems.

338 *2.5.2.1. Binding Free Energy Calculations*

339 The MMPB/GBSA methods, integrated in AMBER 18, were employed to calculate the binding

340 free energies for all six systems (Miller III et al., 2012). Binding free energy calculations were

341 performed on 100 snapshots taken from the MD trajectories as described previously by Abro and

342 Azam (Abro and Azam, 2016). The binding free energy can be expressed as:

343 $\Delta G_{bind} = \Delta G_{complex} - [\Delta G_{receptor} + \Delta G_{ligand}]$

344 where ΔG is the Gibb's free energy calculated by MMGB/PBSA.

345 *2.6. Statistical analysis*

346 The data were analyzed statistically utilizing Graph Pad Prism Software, version 5, for manifold

347 assessments via one-way analysis of variance (ANOVA) with Post-hoc Dunnett's test. Outcomes

348 were regarded as statistically significant at $P < 0.05$.

349 **3. Results**

350 *3.1. In vitro activities*

351 All enzyme suppression results are presented as the mean of triplicate determinations for each

352 concentration studied and an IC_{50} value was extrapolated from the overall inhibitory concentration

353 relationships.

354

355

3.1.1. 5-LOX inhibitory activity

The 5-LOX inhibitory activity of CHD was examined at various concentrations ranging from 31.25

to 1000 µg/ml and the compound displayed a potent inhibition of 5-LOX with an extrapolated IC_{50}

value of 10. 27 µg/ml as compared to the standard 5-LOX inhibitor drug zileuton (extrapolated

$IC_{50} = 5.50$ µg/ml) over the same tested concentration range (Table 2).

3.1.2. COX-2 inhibitory activity

CHD disclosed a potent inhibitory action on the COX-2 enzyme as shown in Table 3. It was also

evident from the outcomes that CHD possessed valuable COX-2 inhibitory activity in comparison

with the standard COX-2 inhibitor drug celecoxib. Thus, the IC_{50} value for CHD was extrapolated

as 8.94 µg/ml in contrast to that of celecoxib ($IC_{50} = 4.30$ µg/ml) (Table 3).

Table 2

5-LOX enzyme inhibitory activity of CHD in comparison with zileuton as a standard 5-LOX inhibitor drug.

Compound	Conc. (µg/ml)	% 5-LOX inhibition (Mean ± S.E.M)	Extrapolated IC_{50} µg/ml
Cyclohexenone derivative (CHD)	1000	89.44 ± 0.55^b	10.27
	500	83.17 ± 0.72^c	
	250	78.30 ± 0.64^c	
	125	73.34 ± 0.63^c	
	62.5	68.30 ± 0.64^c	
	31.25	61.93 ± 1.13^c	
Zileuton	1000	93.55 ± 0.40	5.50
	500	89.37 ± 1.65	
	250	85.50 ± 0.40	
	125	79.60 ± 0.90	
	62.5	74.17 ± 0.72	
	31.25	70.35 ± 0.45	

Data is represented as mean ± S.E.M; Values were significantly different ~~as~~ compared to the positive control (zileuton); n=3, b= $P < 0.01$, c=$P < 0.001$.

371

372

Table 3

COX-2 enzyme inhibitory assay of CHD in comparison with celecoxib as a standard COX-2 inhibitor drug.

Compound	Conc. (µg/ml)	% COX-2 inhibition (Mean ± S.E.M)	Extrapolated IC_{50} µg/ml
Cyclohexenone derivative (CHD)	1000	88.91 ± 1.30^c	8.94
	500	85.00 ± 0.30^c	
	250	78.76 ± 0.58^c	
	125	73.67 ± 0.61^c	
	62.5	67.74 ± 0.61^c	
	31.25	63.47 ± 0.56^c	
Celecoxib	1000	95.20 ± 0.15	4.30
	500	91.17 ± 0.53	
	250	86.98 ± 0.85	
	125	81.20 ± 0.65	
	62.5	77.80 ± 0.37	
	31.25	73.11 ± 1.20	

Data is represented as mean ± S.E.M; Values were significantly different as compared to the positive control (celecoxib); n=3, c=$P < 0.001$.

3.1.3. RT- PCR

To further investigate the anti-inflammatory potential of CHD, RT-PCR was utilized to assess the mRNA levels of COX-2 enzyme and the pro-inflammatory cytokines TNF-α and IL-1β in the carrageenan induced paw edema test in mice. The outcomes of this assessment revealed that CHD (45 mg/kg) significantly reduced the mRNA expression of COX-2 ($P<0.001$), while in the case of TNF-α and IL-1β, CHD also produced a reduction ($P<0.01$) compared to the carrageenan treated vehicle group. Aspirin (150 mg/kg) as the standard positive control decreased ($P<0.001$) the expression of COX-2, TNF-α and IL-1β as presented in (Fig. 2).
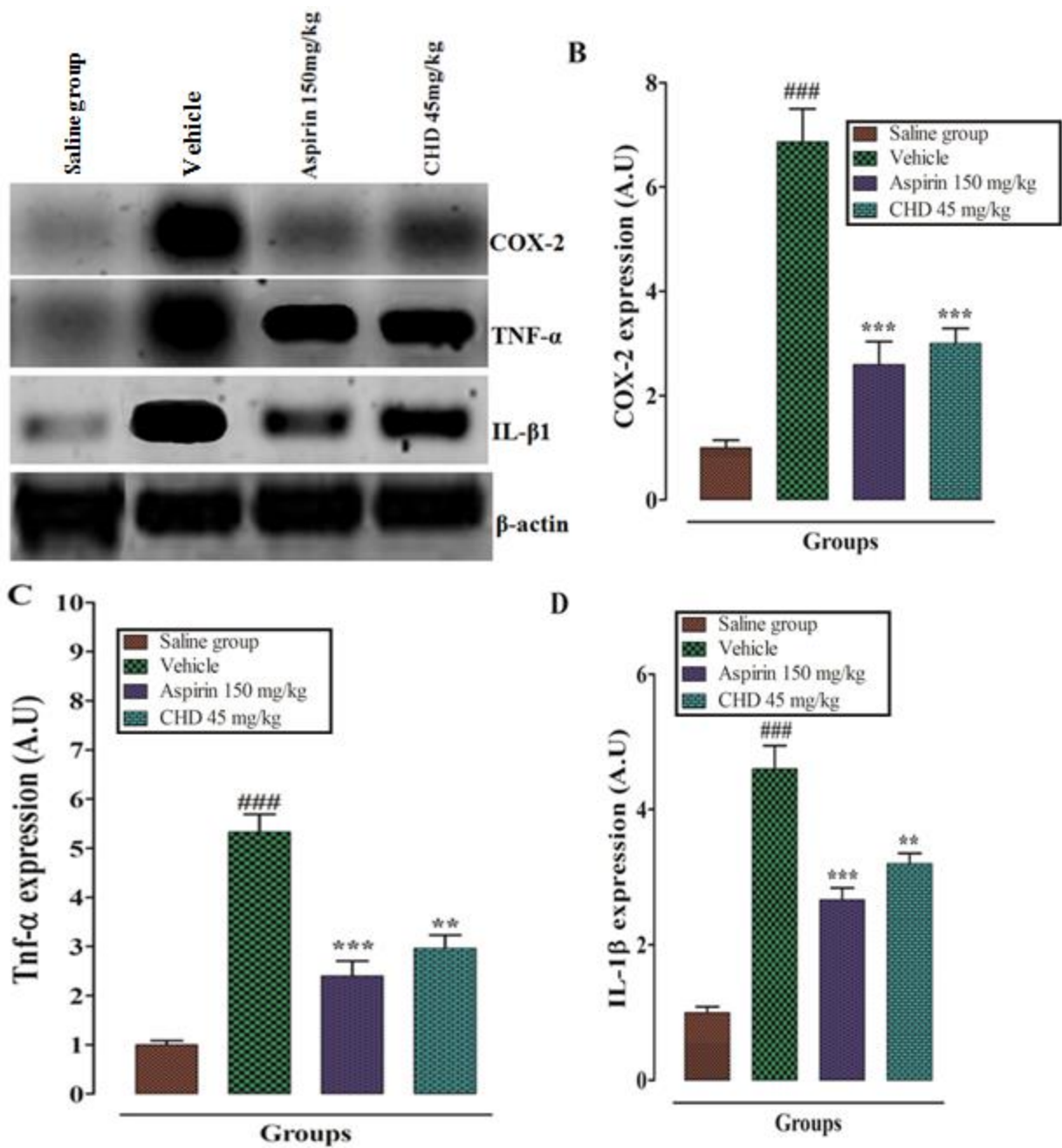
18

Fig. 2. Agarose gel electrophoresis (A) quantification of CHD activity on the mRNA level of COX-2 **(B)**, TNF-α **(C),** and IL-1β **(D)** in carrageenan induced hind paw edema in mice. The results are shown in relative arbitrary units (A.U). Bars represent mean expression in A.U ± S.E.M. ### *P* < 0.001 compared to the saline group. ***P*< 0.01, ****P*< 0.001 compared to the vehicle group.

392

3.2. In vivo pharmacological activity

3.2.1. Acute toxicity of CHD

After i.p. injection of selected doses of CHD (15-240 mg/kg; $n = 6$), there was no acute toxicity observed in gross animal behaviour, neither was any incidence of mortality recorded up to the highest dose. Thus, the maximum tolerated dose (MTD) which was devoid of unacceptable toxicity for CHD was >240 mg/kg.

3.2.2. CHD attenuation of chemically induced tonic nociceptive behaviour

Injection of acetic acid (1%) was accompanied by a significant rise in the nociceptive response perceived as an onset increase in the incidence of abdominal constriction. The percentage protection against this chemically induced tonic nociception in the group of animals treated with CHD at a lower dose (15 mg/kg) decreased the nociceptive response as evidenced by an increase in the percentage protection (44.66%, $P < 0.05$). Likewise, the mid-range CHD dose (30 mg/kg) also protected against acetic acid evoked abdominal constriction (49.78%, $P < 0.01$). and the higher dose (45 mg/kg) had an even greater anti-nociceptive effect (59.81%) reflecting dose dependent activity relative to the saline treated animals. The aspirin positive control also yielded a dose dependant anti-nociceptive response (15-45 mg/kg) versus the saline controls (Fig. 3).

409
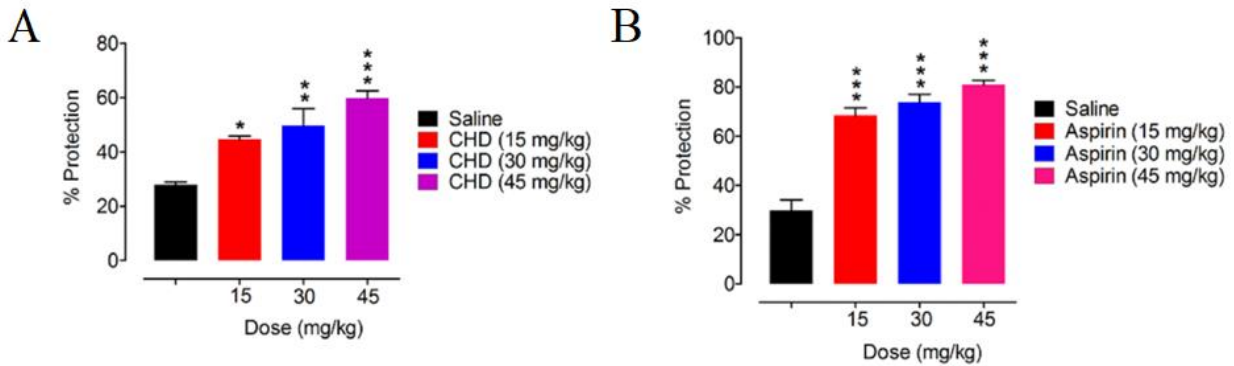
Fig. 3. Anti-nociceptive activity of (A) CHD and (B) the positive control, aspirin in the acetic acid (1%) induced abdominal constriction test. Each bar represents mean percentage protection ± S.E.M). *P< 0.05, **P< 0.01, ***P< 0.001 as compared to the saline treated group (one-way ANOVA followed by *post hoc* Dunnett's test), (*n* = 6 mice per group).

3.2.3. CHD attenuation of phasic thermal nociception

In the hot plate test, the saline treated animal group displayed a control escape response from the thermal nociceptive stimulus of 7.3%, 7.5% and 7.7% after 30, 60 and 90 min respectively. The lower dose of CHD was ineffective in producing any detectable anti-nociception between 30-90 min (19.3%-17.6%). However, CHD at 30 mg/kg did produce an anti-nociceptive effect at 30 min (24.5%) and 60 min (20.8%) but this was not evident after 90 min (19.5%). A greater anti-nociceptive response was noted at the 45 mg/kg dose (27.3%, 24.0% and 20.3% at 30, 60 and 90 min respectively) while the tramadol (30 mg/kg) positive control produced an even bigger response 77.6%, 72.0% and 69.7% at 30, 60 and 90 min respectively (Fig. 4).
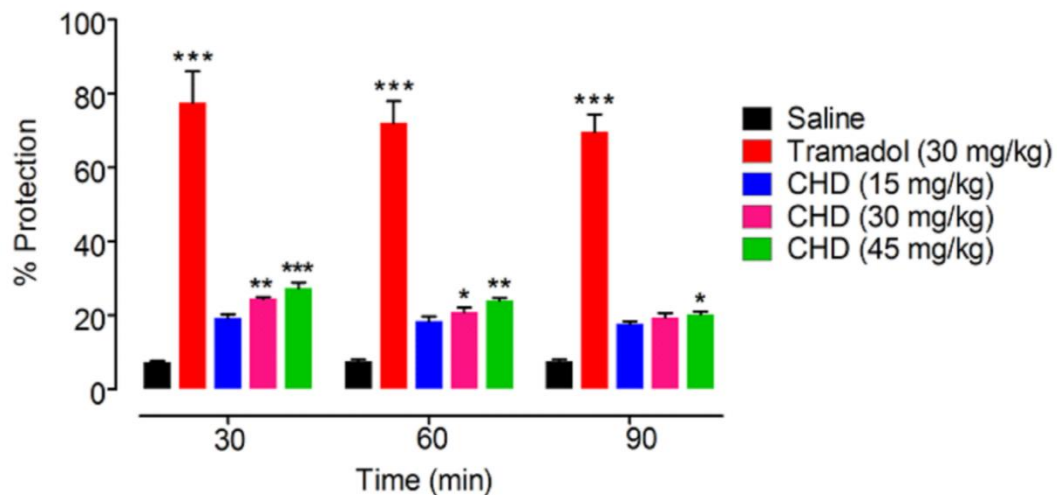
Fig. 4. Anti-nociceptive activity of CHD and the positive control, tramadol, in the hot-plate test. Each bar represents mean percentage protection ± S.E.M). *$P<$ 0.05, **$P<$ 0.01, ***$P<$ 0.001 as compared to saline treated group (one-way ANOVA followed by *post hoc* Dunnett's test), ($n=6$ mice per group).

3.2.4. CHD attenuation of phasic nociception in the tail immersion test
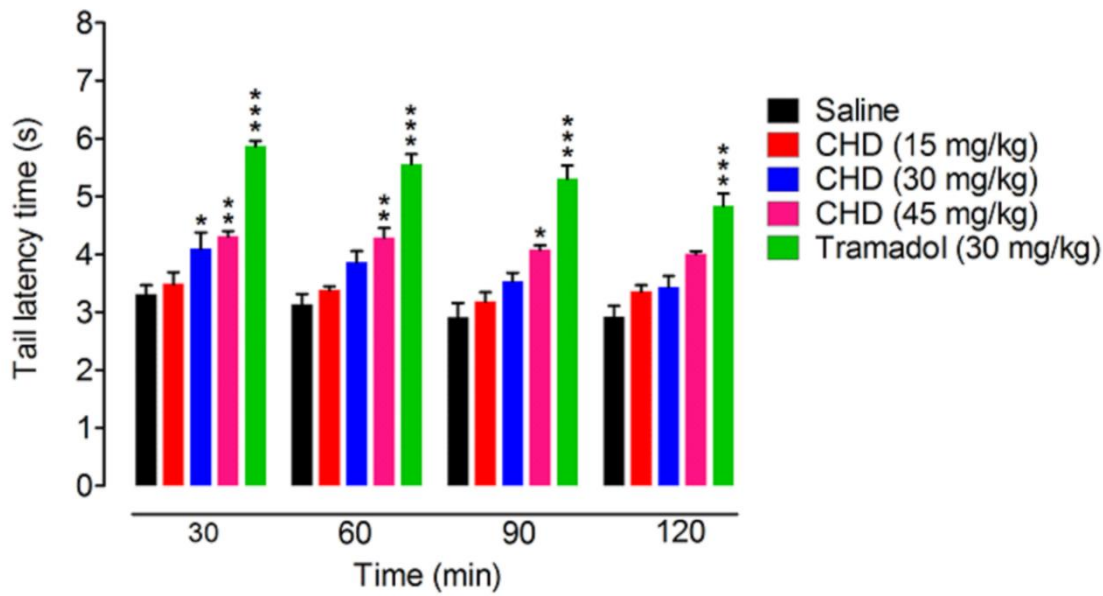
CHD produced a measurable anti-nociceptive response in the tail immersion test at the 30 mg/kg dose (30 min). However, the 45 mg/kg dose produced a peak response at 60 min which subsided by 120 min. Treatment with the positive tramadol control (30 mg/kg), produced an intense long-acting anti-nociceptive effect which lasted up to 120 min (Fig. 5).

434

Fig. 5. Anti-nociceptive activity of CHD and the positive control, tramadol in the thermal tail immersion test. Each bar represents mean withdrawal latency time in s ± S.E.M). ***P< 0.05, **P<** 0.01, *****P< 0.001** as compared to saline treated group (one-way ANOVA followed by *post hoc* Dunnett's test), (*n* = 6 mice per group).

3.2.5. CHD attenuation of the formalin induced biphasic nociceptive response

Administration of formalin in the sub-plantar mouse hind paw initiated a marked nociceptive response as indicated by an increase in the duration of biting, licking, lifting and flinching of the affected paw. This was observed throughout the first phase (0-5 min) and also the second phase (15-30 min) following formalin administration in the saline treated animals. Treatment with CHD (15 mg/kg) only diminished the second phase of formalin induced nociception. Conversely, the 30 mg/kg CHD dose was more effective in that it markedly reduced the formalin nocifensive response in both the second and first phases (*P*< 0.05). Similarly, treatment with the higher CHD dose (45 mg/kg) did induce an anti-nociceptive response in the first phase, but a more statistically

23

448   significant response in the second phase. The indomethacin and diclofenac positive controls both

449   at 10 mg/kg generated comparable anti-nociception to CHD in both phases (Fig. 6).
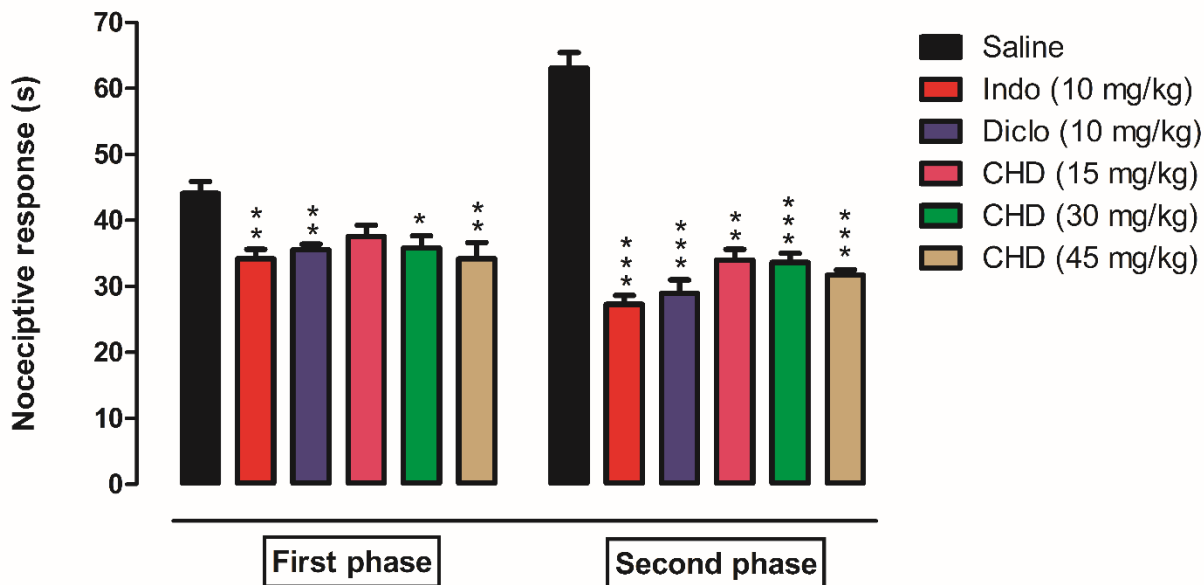
450

451   **Fig. 6.** Anti-nociceptive activity of CHD and the positive controls, indomethacin (Indo), and

452   diclofenac (Diclo) in the formalin induced paw nociceptive test. Each bar represents mean

453   nociceptive response in s ± S.E.M). *$P< 0.05$, **$P< 0.01$, ***$P< 0.001$ as compared to the saline

454   treated group (one-way ANOVA followed by *post hoc* Dunnett's test), ($n = 6$ mice per group).

455   *3.2.6. Opioidergic and GABAergic mediation of CHD anti-nociception*

456   Any possibility of GABAergic or opioidergic mechanisms underlying the anti-nociceptive effect

457   of CHD in the hot-plate test were probed using pentylenetetrazole (PTZ) and naloxone as

458   respective antagonists. Hence, the anti-nociceptive effect of CHD (30 and 40 mg/kg), was

459   significantly antagonized ($P< 0.001$) by naloxone (1 mg/kg) implicating the involvement of an

460   opioidergic mechanism. Likewise, in animals treated with the opioid agonist, tramadol (30 mg/kg)

461   as a positive control, naloxone also blocked the anti-nociceptive response (Fig. 7A).

462   Administration of PTZ (15 mg/kg) did not modify the ani-nociceptive action of tramadol (30

463   mg/kg), but it did markedly decrease the anti-nociceptive response of CHD (30 and 45 mg/kg) in

464   the hot plate paradigm. This would tend to suggest an involvement of a GABAergic mechanism

465   in the anti-nociceptive action of CHD but not tramadol (Fig. 7B).

466
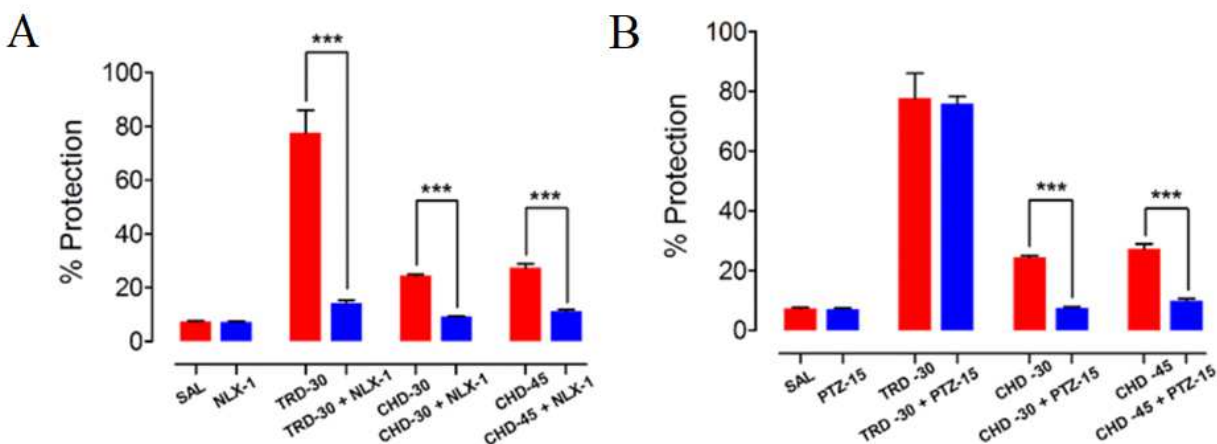
Fig. 7. (A) Effect of naloxone at 1 mg/kg (NLX-1) and (B) PTZ at 15 mg/kg (PTZ-15) on the anti-

468   nociceptive activity of CHD (30 mg/kg, CHD-30 and 45 mg/kg, CHD-45) or tramadol (30 mg/kg,

469   TRD-30) in the mouse hot-plate test. Each bar represents mean percentage protection ± S.E.M.

470   ***$P < 0.001$ compared to saline control (SAL). (two sample t-test), ($n = 6$ mice per group).

471   *3.2.7. Anti-inflammatory action of CHD against phlogistic agents (carrageenan, histamine, and*
472   *serotonin) in the paw volume inflammation and xylene in the ear inflammation test*

473

474   Intraplantar administration of the phlogistic agents, carrageenan, histamine, and serotonin was

475   associated with a pronounced inflammatory response manifested by a substantial increase in the

476   paw volume. The increased edema formation followed a temporal pattern and was first expressed

477   during the initial h of the paradigm and maintained throughout the advanced stages of

478   inflammation i.e. up to 5 h of the study duration. A dose dependent anti-inflammatory effect was

479   produced by CHD in the three paradigms of paw edema. Treatment with CHD (15, 30 and 45

480   mg/kg) reduced the inflammatory response evoked up to 5 h after administration of carrageenan

481   (Fig. 8A), histamine (Fig. 9A), and serotonin (Fig. 10A), Treatment with the aspirin positive

482   control, (50-150 mg/kg) consistently displayed an anti-inflammatory effect up to 5 h after injection

483   of carrageenan, serotonin or histamine in the inflammatory paradigms (Figs 8B, 9B and 10B).

484   In the xylene provoked ear inflammatory edema paradigm, application of xylene produced a

485   marked inflammatory response as observed by the increased ear weight recorded in the saline

486   treated control animals (Fig 11). This marked oedematous change was significantly countered by

487   treatment with CHD (30 and 45 mg/kg). The positive anti-inflammatory control drugs,

488   indomethacin (10 mg/kg) and diclofenac (15 mg/kg) both produced a noteworthy decline in the

489   augmented ear weight edema induced by xylene, as compared to the saline treated controls (Fig.

490   11).
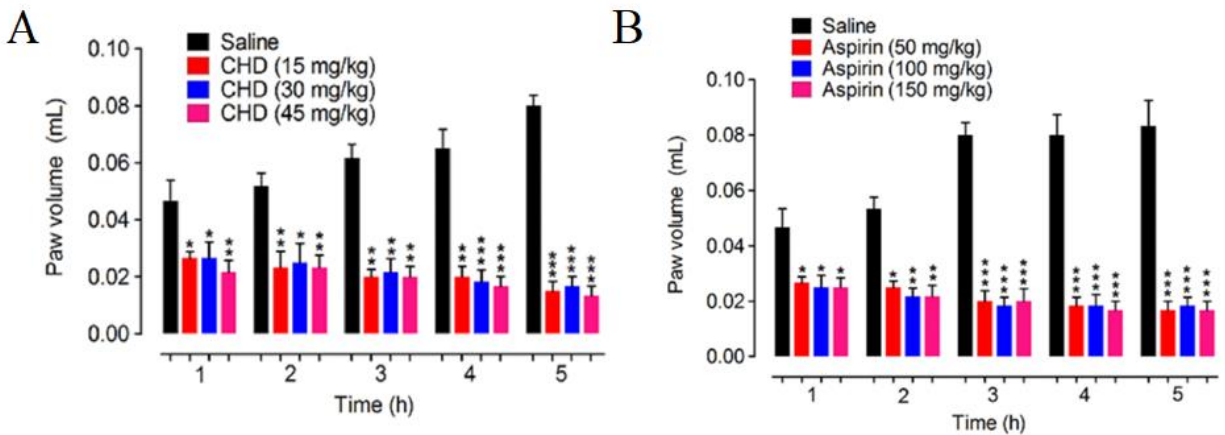
491

492   **Fig. 8.** Anti-inflammatory activity of (A) CHD and (B) the positive control, aspirin in the

493   carrageenan induced paw edema test. Each bar represents paw volume in ml ± S.E.M. *$P< 0.05$,

494   **$P< 0.01$, ***$P< 0.001$ as compared to saline treated group (one-way ANOVA followed by *post*

495   *hoc* Dunnett's test), ($n = 6$ mice per group).

Fig. 9. Anti-inflammatory activity of (A) CHD and (B) the positive control, aspirin in the histamine induced paw edema test. Each bar represents paw volume in ml ± S.E.M. *$P < 0.05$, **$P < 0.01$, ***$P < 0.001$ as compared to saline treated group (one-way ANOVA followed by *post hoc* Dunnett's test), ($n = 6$ mice per group).
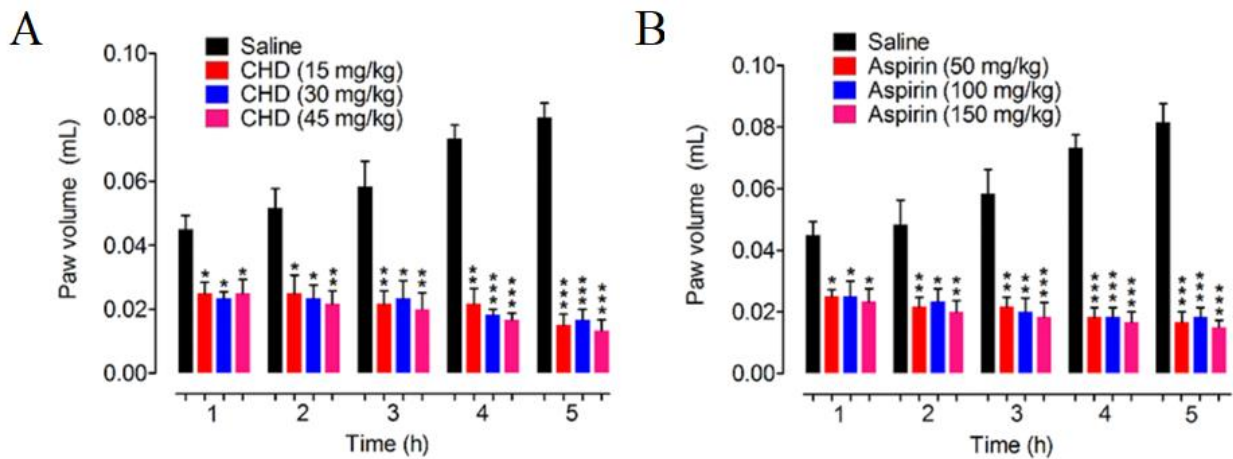

Fig. 10. Anti-inflammatory activity of (A) CHD and (B) the positive control, aspirin in the serotonin induced paw edema test. Each bar represents paw volume in ml ± S.E.M. *$P < 0.05$, **$P < 0.01$, ***$P < 0.001$ as compared to saline treated group (one-way ANOVA followed by *post hoc* Dunnett's test), ($n = 6$ mice per group).

Fig. 11. Anti-inflammatory activity of CHD and the positive controls, indomethacin (Indo), and diclofenac (Diclo) in the xylene induced ear edema test. Each bar represents ear weight in mg ± S.E.M. *$P < 0.05$, **$P < 0.01$, ***$P < 0.001$ compared to the saline treated group (one-way ANOVA followed by *post hoc* Dunnett's test), ($n = 6$ mice per group).
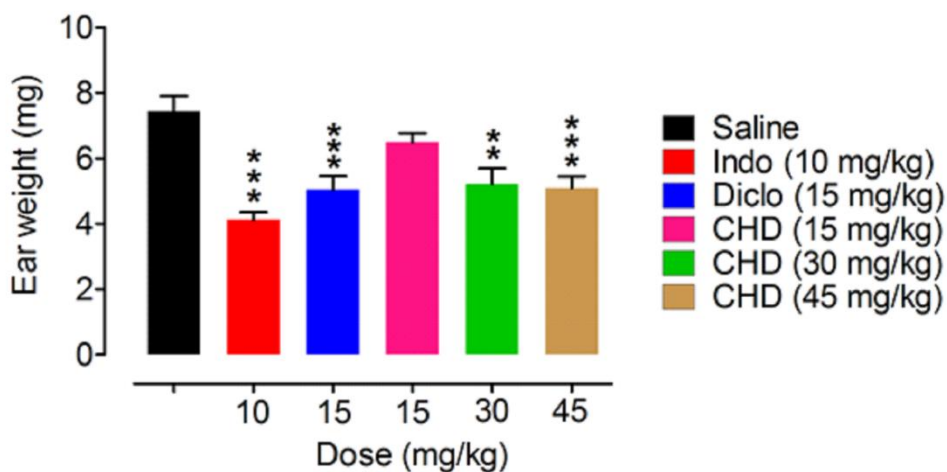
3.3. In silico studies

3.3.1. Molecular Docking

Docking studies were performed to explore any possible underlying mechanism(s) of CHD anti-nociception and anti-inflammatory activity. Accordingly, simulations were carried out on: (1) cyclooxygenase-2 enzyme (COX-2), (2) GABA receptors and (3) opioid μ-, δ- and κ- receptors using Molecular Operating Environment (MOE 2016.08, Chemical Computing Group, Canada). Data concerning three-dimensional (3D) structures of enzymes with their co-crystalized ligands were downloaded from the Protein Data Bank (PDB) listed in Table 1 and the docking algorithm was validated by re-docking native co-crystalized ligands (Table 1). The computed root mean

523   square deviation (RMSD) between experimental and re-docked poses was found to be within a

524   threshold limit < 2 Å.

525   The binding orientation of CHD and the native ligand into the binding site of the COX-2 isoform

526   is shown in Figure 12A. The three-dimensional (3-D) interaction plot of CHD showed that the

527   methoxy group formed a hydrogen bond interaction with His90, an important residue of a

528   selectivity pocket. The carbonyl oxygen formed hydrogen bond interactions with Ala527 (Figure

529   12B). The computed binding energy for the CHD-COX-2 complex was -8.1050 kcal/mol and the

530   docking score was -12.0458.

531
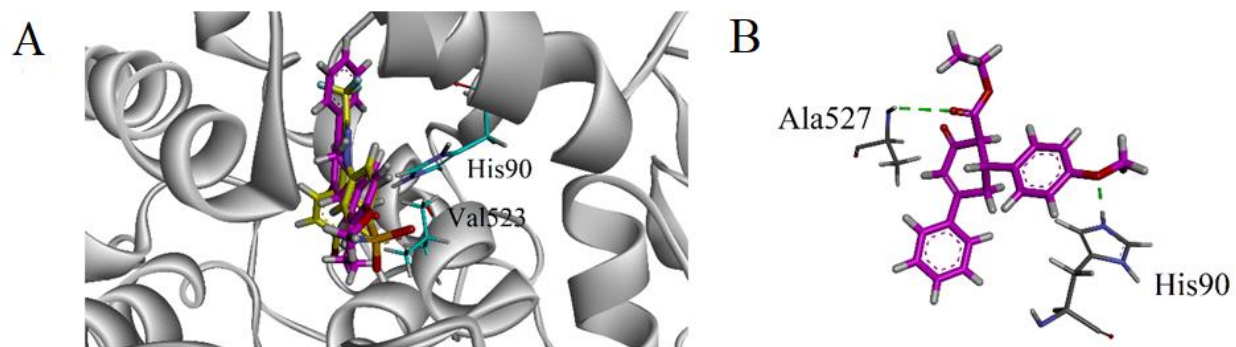
532

533   **Fig. 12. (A)** Ribbon diagram of overlaid binding orientation of CHD and native ligand into the
534   binding site of the COX-2 enzyme. **(B)** Three-dimensional ligand-enzyme interaction plots of the
535   cyclohexenone derivative (CHD) into the binding site of COX-2 enzyme.

536

537   For the GABA receptor, the docking study was carried out on PDB code 4COF (benzamidine).

538   The computed binding energy for the ligand-GABA$_A$ complex was obtained as -5.4853 kcal/mol

539   with a docking score of -8.4314. The superimposed three-dimensional ribbon model of the CHD,

540   (purple), methaqualone (orange) (a positive allosteric GABA$_A$ receptor modulator) and native

541 ligand benzamidine (yellow) is shown in (Fig. 13). The 2D interaction plot showed that the phenyl

542 ring of the synthesized compound creates π-π assembling interactions with Tyr62.
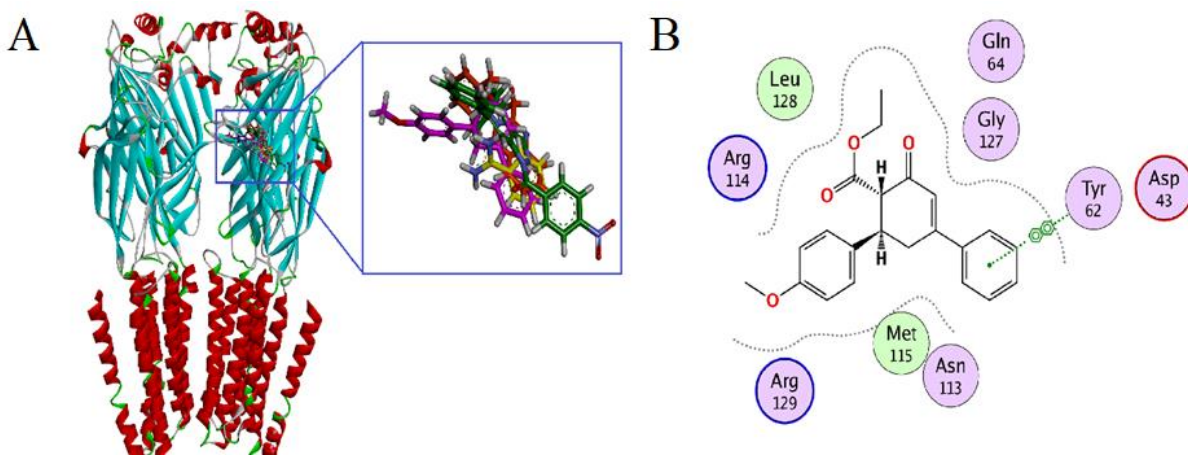
543

544 **Fig. 13.** (**A**) Three-dimensional superimposed binding pose of the native ligand benzamidine
545 (yellow), cyclohexenone derivative (CHD; purple) and methaqualone (orange) into the binding
546 site of the GABA$_A$ receptor (PDB code 4COF) and (**B**) Two-dimensional interaction plot for CHD.

547

548 For μ-opioid receptors (μOR), the computed binding affinity for the ligand-receptor complex was

549 -7.0501 kcal/mol and the docking score was computed as -11.4240 (Fig. 14). μOR are important

550 opioid receptors for pain perception and are currently the target of various potent centrally-acting

551 analgesic drugs. The binding pose of CHD (purple) overlaid with β-funaltrexamine is shown in

552 (Fig. 14). The ligand enzyme complex was stabilized by hydrophobic and π-sulfur interactions.

553 The phenyl ring formed π-π stacking interactions with Tyr326, while the 4-methoxyphenyl group

554 formed π-sulfur interactions with Met151.

555 The binding affinity and docking score in the case of the κ-opioid ligand-receptor complex was

556 calculated as -8.0501 kcal/mol and -12.0240, respectively. The binding pose of the synthesized

557 compound (purple) into the κ-opioid receptor active site (PDB code 4DJH) is shown in Fig. 14.

558 CHD exhibited a binding pose similar to that of the co-crystalized ligand (JDC). The 3D interaction

559 plot showed that the ligand-enzyme complex was stabilized by a hydrogen bond, hydrophobic, π-

560   sulfur   as well as π-CH type interactions. Met142 formed π-sulfur interactions with the 4-

561   methoxyphenyl ring. The phenyl ring of CHD engages in π-π stacking interactions with Trp287.

562   A hydrogen bonding interaction was found between the carbonyl oxygen of the ring with Tyr312.

563   Similarly, Val108, Val230, Val290, Ile294 and Ile316 formed some π-alkyl interactions.

564   For the δ-opioid receptor, the binding affinity for the ligand-enzyme complex was calculated as -

565   7.4000 kcal/mol and the docking score was noted as -11.0903. In the case of δ-opioid receptors,

566   the 3D structure with naltrindole as co-crystalized ligand was retrieved (PDB code = 4EJ4). The

567   superimposed 3D binding pose of CHD (purple) with naltrindole (yellow) is shown in (Fig. 14).

568   The two-dimensional interaction plot showed that it interacted with Met132 *via* hydrogen bond

569   donor interactions.

570

Fig. 14. Three and Two dimensional models of CHD binding with opioid receptors. (**A**) Three-dimensional and (**B**) Two-dimensional modeled superimposed binding pose of native ligand and CHD (purple) into the binding site of δ-opioid receptors (PDB code = 4EJ4). (**C**) Three-dimensional and (**D**) Two-dimensional model superimposed binding pose of native ligand and CHD (purple) into the binding site of κ-opioid receptor (PDB code = 4DJH). (**E**) Three-dimensional and (**F**) Two-dimensional model superimposed binding pose of the native ligand and selected compound CHD (purple) into the binding site of μ-opioid receptors (4DKL).

3.3.2. Molecular Dynamics (MD) Simulations

MD simulations were performed in order to understand the dynamics of all complexes and check the stability of the CHD conformation at the docked site with respect to the backbone atoms for each receptor. Among the complexes, 4COF, 1CX2, and 1EQG showed good stabilty in the presence of CHD compared to the other three receptors (Fig. 15A). The mean RMSDs of these were 2.0 Å, 2.4 Å, and 2.9 Å, respectively. These sites in the presence of CHD at the docked position revealed very constant RMSD patterns throughout the simulaiton time, indicating a good intermolecular strength of affinity and stability pattern. 4DJH (mean RMSD = 6.8 Å), 4DKL (mean RMSD = 5.4 Å), and 4EJ4 (mean RMSD = 4.6 Å) showed major fluctuations in the receptor structures, however, these changes do not affect the binding and conformation of the compound with the receptors. In essence, these RMSD receptor fluctuations correspond to local protein structure movments which are normal to their function. To substantiate compound conformation stability, we additionally computed compound RMSDs in all complexes and plotted them versus time. As can be seen in (Fig. 15B), the compounds were significantly stable with all receptor RMSDs < 1 Å in all frames of the MD simulation.

A
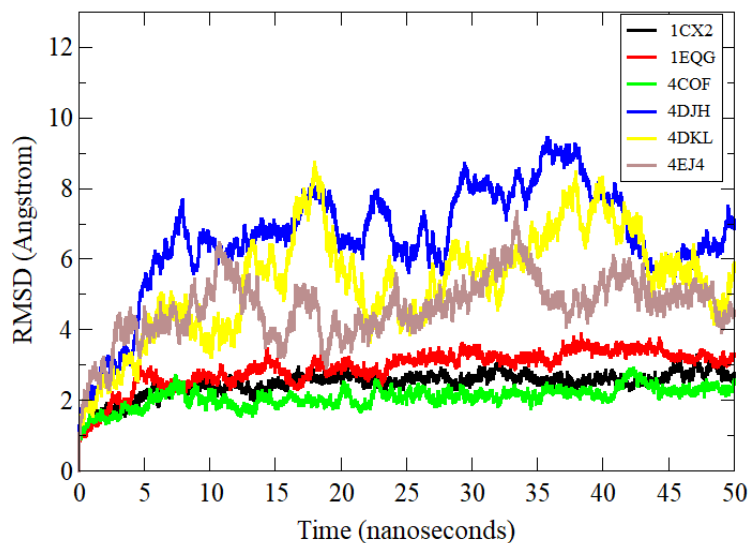
B
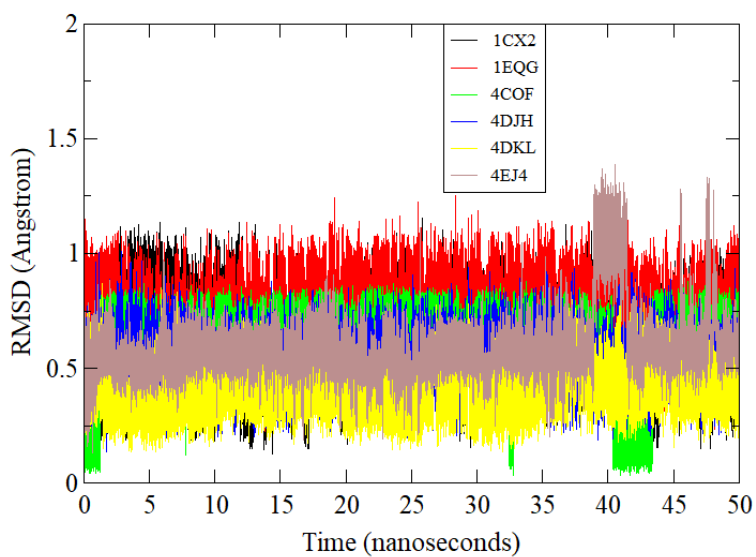
595

Fig. 15. (**A**) Root Mean Square Devitaions of backbone atoms for each receptor of docked complexes. (**B**) CHD Root Mean Square Devitaions over 50-ns of MD simulation in complex with receptors.

599

600

601

3.3.1. MMPB/GBSA Binding Energy Calculation

The free energy of binding was computed for all complexes to evaluate and revalidate the affinity
of intermolecular interactions and discover which type of interaction energy was dominant in
contributing to complex stability. All the complexes divulged robust interaction energies and were
dominated by gas phase energy in both MMGBSA and MMPBSA methodologies. Solvation
energy appeared to play less of a role in molecular interactions and was therefore non-favorable.
More specifically, the van der Waals energy of the gas phase disclosed by both methods played a
key role in complex stability whereas a minor contribution from electrostatic energy was also
evident except in the case of ICX2.The non-polar energy of solvation also favored docked
molecules as opposed to a highly unfavorable contribution from polar solvation energy. Overall,
the 4DKL receptor in complex with the CHD compound was highly stable with a MMGBSA
energy of -55.4492 kcal/mol and -47.9865 kcal/mol in MMPBSA. Details of MMGBSA and
MMPBSA energies of the complexes can be viewed in Table 4.

615

616 **Table 4**

617 MMGBSA and MMPBSA binding energies of the complexes

Method	Energy Component	1EQG	1CX2	4COF	4DKL	4EJ4	4DJH
MMGBSA	VDWAALS	-40.4511	-52.1322	-47.2564	-62.2517	-61.1760	-53.3142
	EEL	-6.2952	3.4110	-25.3784	-8.2760	-10.7373	-9.9464
	EGB	18.2375	8.9329	35.5743	21.3416	24.9894	19.8313
	ESURF	-4.3177	-5.6008	-4.8037	-6.2631	-6.2177	-5.5521
	DELTA G gas	-46.7463	-48.7212	-72.6348	-70.5277	-71.9133	-63.2606
	DELTA G solv	13.9198	3.3320	30.7706	15.0785	18.7716	14.2792
	DELTA TOTAL	-32.8265	-45.3892	-41.8641	-55.4492	-53.1417	-48.9814
MMPBSA	VDWAALS	-40.4511	-52.1322	-47.2564	-62.2517	-61.1760	-53.3142
	EEL	-6.2952	3.4110	-25.3784	-8.2760	-10.7373	-9.9464
	EPB	22.4009	14.6505	40.4885	26.2948	32.7712	26.3717
	ENPOLAR	-2.9491	-3.5859	-3.3982	-3.7537	-3.7336	-3.6908
	EDISPER	0.0000	0.0000	0.0000	0.0000	0.0000	0.0000
	DELTA G gas	-46.7463	-48.7212	-72.6348	-70.5277	-71.9133	-63.2606
	DELTA G solv	19.4518	11.0646	37.0904	22.5411	29.0376	22.6810
	DELTA TOTAL	-27.2945	-37.6567	-35.5444	-47.9865	-42.8757	-40.5796

618

619

620 **4. Discussion**

621 Cyclohexenone derivatives have received considerable attention over recent years not only

622 preclinically, but also clinically because of their extensive pharmacological possibilities. These

623 include: analgesic (Said et al., 2009), anti-inflammatory (Yaouba et al., 2018), anti-neuropathic

624 (Khan et al., 2019), antipyretic (Mousavi, 2016), antibacterial (Saranya and Ravi, 2012),

625 antioxidant (Okoth et al., 2016), antifungal (Kanagarajan et al., 2013), antimalarial (Ledoux et al.,

626 2017), anti-tubercular (Monga et al., 2014), anti-leishmanial (Das and Manna, 2015),

627 anticonvulsant (Said et al., 2009) tyrosine kinase inhibitory (Nazar et al., 2015) cytotoxic (Ayyad

628 et al., 1998) and anticancer (Okoth and Koorbanally, 2015) activities. Bearing in mind these wide-

629 ranging potential capacities of cyclohexenone functionality, this study was designed to examine a

630 selected cyclohexanone derivative (CHD) exemplar (Ethyl 6-(4-metohxyphenyl)-2-oxo-4-

631 phenylcyclohexe-3-enecarboxylate). This was done firstly for its safety profile; secondly, to

632 investigate any feasible *in vivo* effects in standard animal models of nociceptive and inflammatory

633 pain; thirdly, to perform molecular docking and molecular dynamic (MD) simulation studies to

634 facilitate interpretation of targeted drug-receptor interactions to corroborate the *in vivo* findings.

635 In parallel with this research approach, *in vitro* assays were conducted to examine any possibility

636 of COX-2 or 5-LOX enzyme inhibition and/or suppression of mRNA expression of TNF-α, IL-1β

637 and COX-2 that might underlie anti-nociceptive and anti-inflammatory effects.

638   Four nociceptive and inflammatory, highly reproducible standard models were used to generate

639 the results. The findings clearly indicated that CHD possessed a noteworthy degree of safety with

640 a maximum tolerated dose above 240 mg/kg. Statistically significant anti-nociceptive and anti-

641 inflammatory activity was found in the rodent models. These effects were comparable to those of

642 aspirin, tramadol, indomethacin and diclofenac used as positive controls (Figs. 3, 4, 5, 6, 7, 8, 9,

643 10 and 11). Moreover, *in silico* docking analysis demonstrated that CHD manifested

644 favorable interactions with common pain targets i.e. COX-1/2 enzymes in addition to opioid and

645 GABA$_A$ receptors (Figs. 12, 13 and 14.) substantiating the in-vivo results. Equally, CHD produced

646 marked inhibition of COX-2 and 5-LOX in the enzyme assays while in the case of RT-PCR, CHD

647 reduced the mRNA expression of TNF-α, IL-1β and COX-2.

648   Administration of GABA receptor agonists either supraspinally, spinally or peripherally, has

649   been reported to reduce the nociceptive index in models of neuropathic and inflammatory pain

650   (Malan et al., 2002; Patel et al., 2001). In our study, it is postulated that CHD alleviates centrally

651   mediated nociception via GABAergic and opioidergic mechanisms (Fig. 7) alongside a capability

652   of interaction with the COX-1/2 target (Fig. 12). An involvement of GABAergic and opioidergic

653   systems was further reinforced by computational studies whereby CHD exhibited favorable

654   binding affinity for the $GABA_A$ (Fig. 13) and opioid receptor subtypes (μ, κ and δ) (Fig. 14).   It

655   has been reported that GABAergic agonists may augment the anti-nociceptive effect of a centrally

656   acting analgesic such as morphine (Sawynok, 1984), hence, it is conceivable that GABA receptor

657   agonist administration may represent a therapeutic option for the management of both chronic and

658   acute pain (McCarson and Enna, 2014) or as a combination of GABA with opioid receptor related

659   therapies.

660   The acetic acid induced abdominal constriction assay is a tonic visceral pain model frequently

661   utilized for monitoring the anti-nociceptive action of drugs (Utsunomiya et al., 1998). Although it

662   is a very sensitive test, it cannot distinguish whether the nociceptive activity is peripherally or

663   centrally mediated (Chen et al., 1995). It entails stimulation of visceral receptors followed by the

664   release of bradykinin, serotonin, cyclooxygenase, prostaglandins and interleukins which induce

665   pain and inflammation (Olonode et al., 2015; Rodrigues et al., 2012). It also implicates an

666   enhanced activation of peripheral receptors (Bentley et al., 1983) and innervated nociceptive nerve

667   terminals (Duarte et al., 1988). In the current study, CHD induced a significant reduction in

668   abdominal constrictions in a dose-dependent manner comparable to standard aspirin (Fig. 3A-B).

669   Hot plate and tail immersion nociceptive tests were employed to determine the central anti-

670   nociceptive potential of CHD. These models can specifically evaluate possible central nociception

671 (Eddy and Leimbach, 1953), where there is a non-inflammatory and acute nociceptive reaction

672 developed upon exposure to heat via spinal receptors which is evidence of centrally mediated anti-

673 nociception (Amabeoku and Kabatende, 2012; Pini et al., 1997). CHD moderately enhanced the

674 hot plate latencies of mice compared to standard tramadol, suggesting it to be a centrally acting

675 analgesic (Fig. 4). In the tail immersion test, the behavioural response is predominantly controlled

676 by supraspinal and spinal entities (Danneman et al., 1994). At the doses studied, CHD presented a

677 modest increase in tail withdrawal latency, but tramadol produced a more pronounced latency

678 elevation (Fig. 5). The duration of action of a drug depends on several factors including biological

679 half-life, first pass effect, plasma protein binding and other pharmacokinetic factors, nature of

680 formulation, co-morbid conditions such as renal impairment or liver disfunction. Any of the above

681 cited factors, may be a potential contributor to the loss of CHD effectiveness at the doses of 30

682 and 45 mg/kg in the thermal nociception tests within 90 min (hot plate test) and 120 min (tail

683 immersion test), respectively. The formalin induced nociceptive paradigm comprises of a binary

684 phased nociceptive reaction and neuropathic pain (Salinas-Abarca et al., 2017). A neurogenic or

685 first phase (0-5 min) in which class C fibres are stimulated and an inflammatory or second phase

686 (10 to 30 min) which involves the release of inflammatory mediators (Hunskaar and Hole, 1987;

687 Tjølsen et al., 1992). Interestingly, CHD was effective in both the neurogenic and inflammatory

688 mediator phases (Fig. 6), further reinforcing the concept of a possible centrally acting anti-

689 nociceptive component mechanism in the activity of this compound. Moreover, in experiments

690 involving pharmacological antagonism of CHD anti-nociception with PTZ and naloxone, it was

691 divulged that an apparent participation of both GABAergic and opioidergic mechanisms was

692 implicated (Fig. 7A-B).

693   The anti-inflammatory activity of CHD was investigated by employing four standard models

694   of inflammation i.e., the carrageenan, serotonin, histamine and xylene mediated edema tests (Figs.

695   8, 9, 10 and 11). The carrageenan incited paw volume model is most extensively employed for

696   evaluating the anti-edematous potential of drugs (Mazzanti and Braghiroli, 1994). Localised paw

697   injection of carrageenan in mice initiates a three-phased inflammatory process. The primary phase

698   (0 to 1.5 h), is caused by the release of serotonin and histamine whereas the secondary phase (1.5

699   to 2.5 h) is mediated via bradykinin and the tertiary phase (2.5 to 5 h) is elicited mainly by the

700   generation of prostaglandins (Suba et al., 2005).

701   CHD (15 - 45 mg/kg) substantially reduced the elevated paw edema in all three phases of the

702   carrageenan-induced paw volume assay and this was comparable to the response yielded by the

703   standard drug, aspirin (Fig 8A-B). In order to authenticate the finding from the carrageenan paw

704   edema model, the anti-edematous effect of CHD was further investigated in the three other

705   standard models (histamine and serotonin induced paw volume and xylene induced ear edema).

706   Histamine and serotonin can increase vascular permeability and both are effective vasodilators

707   (Skidmore and Whitehouse, 1967) which are conducive to an ensuing edema. CHD not only

708   suppressed the edema mediated by histamine and serotonin but also that of xylene at doses

709   corresponding to standard anti-inflammatory drugs (Figs. 9A-B, 10A-B and 11). The xylene

710   induced ear edema model is extensively utilized to determine the anti-inflammatory action of

711   steroidal and non-steroidal anti-phlogistic agents (Zanini Jr et al., 1992). Studies reported in the

712   literature have revealed that xylene also promotes vascular permeability causing skin edema owing

713   to the release of inflammatory mediators leading to acute neurogenic inflammation (Bánki et al.,

714   2014). CHD markedly reduced ear edema induced by xylene comparable to the standard agents

715   (Fig. 11).

716   To further corroborate the anti-nociceptive and anti-inflammatory potential of CHD, it was

717   subjected to *in vitro* studies involving 5-LOX and COX-2 enzyme inhibition assays along with

718   RT-PCR studies. Thus, CHD substantially inhibited 5-LOX and COX-2 enzymes in comparison

719   with the standard inhibitors zileuton and celecoxib respectively as shown in (Table 2 and 3). In the

720   case of RT-PCR studies, CHD decreased the mRNA expression of COX-2, TNF-α and IL-1β

721   compared to the carrageenan treated control group as presented in Fig. 2. This *in vitro* study

722   therefore endorsed the promising anti-nociceptive and anti-inflammatory findings with CHD in

723   both the *in vivo* and *in silico* studies which further strengthens a potential for application in pain

724   and inflammation.

725   In summary, *in silico* docking analysis demonstrated that the synthesized cyclohexanone

726   derivative has shown favourable interactions with common pain targets i.e. COX 1/2, GABA$_A$ and

727   opioid receptors (Figs. 12, 13 and 14). The binding affinity study revealed that the intensity of

728   interactions of the CHD ligand with the COX-2 isozyme was more than that with COX-1 and this

729   was supported by the degree of 5-LOX and COX-2 enzyme inhibition observed (Table 2 and 3).

730   In addition, MD simulations of the complexes revealed that CHD was a highly stable molecule at

731   the docked site and generated robust chemical interactions underlying strong intermolecular

732   affinity (Table 4). Interactions with other pharmacological targets suggest that CHD may act as a

733   novel nociceptive and inflammatory pain reliever supported by *in vivo* studies (Figs. 3, 4, 5, 6, 7,

734   8, 9, 10 and 11).

735   **5. Conclusions**

736   This study elucidated the synthesis and pharmacological evaluation of a novel cyclohexenone

737   derivative (CHD) as a putative analgesic agent. CHD possessed not only anti-nociceptive, but also

738   anti-inflammatory activity when tested in validated models of pain and inflammation in mice.

41

739 These *in vivo* properties were attended by an inhibitory action on COX-2 and 5-LOX enzymes *in*

740 *vitro* in addition to a complementary *in silico* interaction with $GABA_A$ and opioid receptors.

741 Consequently, CHD represents an innovative and noteworthy anti-nociceptive and anti-

742 inflammatory compound worthy of further pharmacological investigation and possible

743 development.

752 **Conflict of interest**

753 The authors have no conflict of interest.

754

755 **Authors' contributions**

756 GA conceived the research study and directed the research group as supervisor of the

757 pharmacological experimentation. GA also interpreted the results in addition to critically

758 reviewing the contents of the final version of manuscript. JK carried out the pharmacological

759 experiments and performed the statistical analyses. He likewise developed the preliminary draft of

760 the manuscript. RK helped in planning and supervising experiments related to the chemistry of our

761 selected compound. UR conducted the computational studies and performed related calculations,

762 interpretations and analysis. RU, MSJ, AAK, SA and SA helped in conducting the in vitro and in

763 silico studies. All authors read and approved the final manuscript and RDES had an intellectual

764 input in the writing of the manuscript and the interpretational outcome of the study.

765

766 **References**

767 Abbas, M., Subhan, F., Mohani, N., Rauf, K., Ali, G., Khan, M., 2011. The involvement of opioidergic

768 mechanisms in the activity of Bacopa monnieriextract and its toxicological studies. Afr. J. Pharm.

769 Pharmacol. 5, 1120-1124.

770 Abbasi, S., Raza, S., Azam, S.S., Liedl, K.R., Fuchs, J.E., 2016. Interaction mechanisms of a melatonergic

771 inhibitor in the melatonin synthesis pathway. J. Mol. Liq. 221, 507-517.

772 Abro, A., Azam, S.S., 2016. Binding free energy based analysis of arsenic (+ 3 oxidation state)

773 methyltransferase with S-adenosylmethionine. J. Mol. Liq. 220, 375-382.

774 Ahmad, N., Subhan, F., Islam, N.U., Shahid, M., Rahman, F.U., Sewell, R.D.J.E.j.o.p., 2017. Gabapentin and

775 its salicylaldehyde derivative alleviate allodynia and hypoalgesia in a cisplatin-induced neuropathic pain

776 model. Eur. J. Pharmacol. 814, 302-312.

777 Ahmadi, A., Khalili, M., Hajikhani, R., Hosseini, H., Afshin, N., Nahri-Niknafs, B., 2012. Synthesis and study

778 the analgesic effects of new analogues of ketamine on female wistar rats. Med. Chem. 8, 246-251.

779 Akbar, S., Subhan, F., Karim, N., Shahid, M., Ahmad, N., Ali, G., Mahmood, W., Fawad, K.J.B.,

780 Pharmacotherapy, 2016. 6-Methoxyflavanone attenuates mechanical allodynia and vulvodynia in the

781 streptozotocin-induced diabetic neuropathic pain. Biomed. Pharmacother. 84, 962-971.

782 Ali, G., Subhan, F., Abbas, M., Zeb, J., Shahid, M., Sewell, R.D., 2015. A streptozotocin-induced diabetic

783 neuropathic pain model for static or dynamic mechanical allodynia and vulvodynia: validation using

784 topical and systemic gabapentin. Naunyn-Schmiedeberg's. Arch. Pharmacol. 388, 1129-1140.

785 Ali, G., Subhan, F., Wadood, A., Ullah, N., Islam, N.U., Khan, I., 2013. Pharmacological evaluation,

786 molecular docking and dynamics simulation studies of salicyl alcohol nitrogen containing derivatives. Afr.

787 J. Pharm. Pharmacol. 7, 585-596.

788 Almeer, R.S., Hammad, S.F., Leheta, O.F., Abdel Moneim, A.E., Amin, H.K., 2019. Anti-inflammatory and

789 anti-hyperuricemic functions of two synthetic hybrid drugs with dual biological active sites. Int. J. Mol. Sci.

790 20, 5635.

791 Amabeoku, G.J., Kabatende, J., 2012. Antinociceptive and anti-inflammatory activities of leaf methanol

792 extract of Cotyledon orbiculata L.(Crassulaceae). Adv. Pharmacol. Sci. 2012, 5-6.

793 Ayyad, S.-E.N., Judd, A.S., Shier, W.T., Hoye, T.R., 1998. Otteliones A and B: Potently cytotoxic 4-

794 methylene-2-cyclohexenones from Ottelia alismoides. J. Org. Chem. 63, 8102-8106.

795 Bánki, E., Hajna, Z., Kemeny, A., Botz, B., Nagy, P., Bolcskei, K., Tóth, G., Reglodi, D., Helyes, Z., 2014. The

796 selective PAC1 receptor agonist maxadilan inhibits neurogenic vasodilation and edema formation in the

797 mouse skin. Neuropharmacology 85, 538-547.

798 Bentley, G., Newton, S., Starr, J., 1983. Studies on the antinociceptive action of α-agonist drugs and their

799 interactions with opioid mechanisms. Br. J. Pharmacol. 79, 125-134.

800 Burnett, B., Jia, Q., Zhao, Y., Levy, R., 2007. A medicinal extract of Scutellaria baicalensis and Acacia

801 catechu acts as a dual inhibitor of cyclooxygenase and 5-lipoxygenase to reduce inflammation. J. Med.

802 Food. 10, 442-451.

803 Case, D., Darden, T., Cheatham III, T., Simmerling, C., Wang, J., Duke, R., Luo, R., Walker, R., Zhang, W.,

804 Merz, K., 2010. AMBER 12; University of California: San Francisco, 2012. There is no corresponding record

805 for this reference.[Google Scholar], 1-826.

806 Chapman, C.R., Gavrin, J., 1999. Suffering: the contributions of persistent pain. Lancet 353, 2233-2237.

807 Chen, Y.-F., Tsai, H.-Y., Wu, T.-S., 1995. Anti-inflammatory and analgesic activities from roots of Angelica

808 pubescens. Planta. Med. 61, 2-8.

809   Cheon, M.S., Yoon, T., Choi, G., Moon, B.C., Lee, A.-Y., Choo, B.K., Kim, H.K., 2009. Chrysanthemum

810   indicum Linné extract inhibits the inflammatory response by suppressing NF-κB and MAPKs activation in

811   lipopolysaccharide-induced RAW 264.7 macrophages. J. Ethnopharmacol. 122, 473-477.

812   Danneman, P.J., Kiritsy-Roy, J.A., Morrow, T.J., Casey, K.L., 1994. Central delay of the laser-activated rat

813   tail-flick reflex. Pain 58, 39-44.

814   Das, M., Manna, K., 2015. Bioactive cyclohexenones: a mini review. Curr. Bioact. Compd. 11, 239-248.

815   DiMasi, J.A., Feldman, L., Seckler, A., Wilson, A., 2010. Trends in risks associated with new drug

816   development: success rates for investigational drugs. Clin. Pharmacol. Ther. 87, 272-277.

817   Duarte, I., Nakamura, M., Ferreira, S., 1988. Participation of the sympathetic system in acetic acid-induced

818   writhing in mice. Braz. J. Med. Biol. Res. 21, 341-343.

819   Eddy, N.B., Leimbach, D., 1953. Synthetic analgesics. II. Dithienylbutenyl-and dithienylbutylamines. J.

820   Pharmacol. Exp. Ther. 107, 385-393.

821   Fang, S.-M., Cui, C.-B., Li, C.-W., Wu, C.-J., Zhang, Z.-J., Li, L., Huang, X.-J., Ye, W.-C., 2012.

822   Purpurogemutantin and purpurogemutantidin, new drimenyl cyclohexenone derivatives produced by a

823   mutant obtained by diethyl sulfate mutagenesis of a marine-derived Penicillium purpurogenum G59. Mar.

824   Drugs. 10, 1266-1287.

825   Fawad, K., Islam, N.U., Subhan, F., Shahid, M., Ali, G., Rahman, F.-U., Mahmood, W., Ahmad, N., 2018.

826   Novel hydroquinone derivatives alleviate algesia, inflammation and pyrexia in the absence of gastric

827   ulcerogenicity. Trop. J. Pharm. Res. 17, 53-63.

828   Fernandes, J.V., Cobucci, R.N.O., Jatobá, C.A.N., de Medeiros Fernandes, T.A.A., de Azevedo, J.W.V., de

829   Araújo, J.M.G., 2015. The role of the mediators of inflammation in cancer development. Pathol. Oncol.

830   Res. 21, 527-534.

831   Gopalakrishnan, M., Thanusu, J., Kanagarajan, V., 2008. Synthesis and characterization of 4, 6-diaryl-4, 5-

832   dihydro-2H-indazol-3-ols and 4, 6-diaryl-2-phenyl-4, 5-dihydro-2H-indazol-3-ols—a new series of fused

833   indazole derivatives. Chem. Heterocycl. Comp. 44, 950-955.

834   Gutthann, S.P., Rodríguez, L.A.G., Raiford, D.S., Oliart, A.D., Romeu, J.R., 1996. Nonsteroidal anti-

835   inflammatory drugs and the risk of hospitalization for acute renal failure. Arch. Intern. Med. 156, 2433-

836   2439.

837   Hunskaar, S., Hole, K., 1987. The formalin test in mice: dissociation between inflammatory and non-

838   inflammatory pain. Pain 30, 103-114.

839   Iftikhar, F., Ali, Y., Kiani, F.A., Hassan, S.F., Fatima, T., Khan, A., Niaz, B., Hassan, A., Ansari, F.L., Rashid, U.,

840   2017. Design, synthesis, in vitro Evaluation and docking studies on dihydropyrimidine-based urease

841   inhibitors. Bioorg. Chem. 74, 53-65.

842   Iftikhar, F., Yoqoob, F., Tabassum, N., Jan, M.S., Sadiq, A., Tahir, S., Batool, T., Niaz, B., Ansari, F.L.,

843   Chaudhary, M.I., 2018. Design, Synthesis, In-Vitro Thymidine Phosphorylase Inhibition, In-Vivo

844   Antiangiogenic and In-Silico Studies of C-6 substituted dihydropyrimidines. Bioorg. Chem. 80, 99-111.

845   Islam, N.U., Amin, R., Shahid, M., Amin, M., Zaib, S., Iqbal, J., 2017. A multi-target therapeutic potential of

846   Prunus domestica gum stabilized nanoparticles exhibited prospective anticancer, antibacterial, urease-

847   inhibition, anti-inflammatory and analgesic properties. BMC. Complement. Altern. Med. 17, 272-276.

848   Islam, N.U., Jalil, K., Shahid, M., Rauf, A., Muhammad, N., Khan, A., Shah, M.R., Khan, M.A., 2019. Green

849   synthesis and biological activities of gold nanoparticles functionalized with Salix alba. Arab. J. Chem. 12,

850   2914-2925.

851   Jan, M.S., Ahmad, S., Hussain, F., Ahmad, A., Mahmood, F., Rashid, U., Ullah, F., Ayaz, M., Sadiq,

852   A.J.E.j.o.m.c., 2020. Design, synthesis, in-vitro, in-vivo and in-silico studies of pyrrolidine-2, 5-dione

853   derivatives as multitarget anti-inflammatory agents. Eur. J. Med. Chem. 186, 111863.

854   Johnson, T., Pultar, F., Menke, F., Lautens, M., 2016. Palladium-Catalyzed α-Arylation of Vinylogous Esters

855   for the Synthesis of γ, γ-Disubstituted Cyclohexenones. Org. Lett. 18, 6488-6491.

856   Jones, R., Rubin, G., Berenbaum, F., Scheiman, J., 2008. Gastrointestinal and cardiovascular risks of

857   nonsteroidal anti-inflammatory drugs. Am. J. Med. 121, 464-474.

858   Kanagarajan, V., Ezhilarasi, M., Bhakiaraj, D., Gopalakrishnan, M., 2013. In vitro anticandidal evaluation of

859   novel highly functionalized bis cyclohexenone ethyl carboxylates. Eur. Rev. Med. Pharmacol. Sci. 17, 292-

860   298.

861   Khalid, S., Ullah, M.Z., Khan, A.U., Afridi, R., Rasheed, H., Khan, A., Ali, H., Kim, Y.S., Khan, S., 2018.

862   Antihyperalgesic properties of honokiol in inflammatory pain models by targeting of NF-κB and Nrf2

863   signaling. Front Pharmacol. 9, 140.

864   Khan, J., Ali, G., Khan, R., Ullah, R., Ullah, S., 2019. Attenuation of vincristine-induced neuropathy by

865   synthetic cyclohexenone-functionalized derivative in mice model. Neurol Sci, 1-13.

866   Kidd, B., Urban, L., 2001. Mechanisms of inflammatory pain. Br. J. Anaesth. 87, 3-11.

867   Laxmaiah Manchikanti, M., Bert Fellows, M., Hary Ailinani, M., 2010. Therapeutic use, abuse, and

868   nonmedical use of opioids: a ten-year perspective. Pain. Physician. 13, 401-435.

869   Lednicer, D., Von Voigtlander, P.F., Emmert, D.E., 1981a. 4-Aryl-4-aminocyclohexanones and their

870   derivatives, a novel class of analgesics. 3. m-hydroxyphenyl derivatives. J. Med. Chem. 24, 341-346.

871   Lednicer, D., VonVoigtlander, P.F., Emmert, D.E., 1981b. 4-Amino-4-arylcyclohexanones and their

872   derivatives: a novel class of analgesics. 2. Modification of the carbonyl function. J. Med. Chem. 24, 404-

873   408.

874   Ledoux, A., St-Gelais, A., Cieckiewicz, E., Jansen, O., Bordignon, A., Illien, B., Di Giovanni, N., Marvilliers,

875   A., Hoareau, F., Pendeville, H., 2017. Antimalarial activities of alkyl cyclohexenone derivatives isolated

876   from the leaves of Poupartia borbonica. J. Nat. Prod. 80, 1750-1757.

877   Liu, D., Yu, W., Li, J., Pang, C., Zhao, L., 2013. Novel 2-(E)-substituted benzylidene-6-(N-substituted

878   aminomethyl) cyclohexanones and cyclohexanols as analgesic and anti-inflammatory agents. Med. Chem.

879   Res. 22, 3779-3786.

880   Malan, T.P., Mata, H.P., Porreca, F., 2002. Spinal GABAAand GABABReceptor Pharmacology in a Rat Model

881   of Neuropathic Pain. Anesthesiology. 96, 1161-1167.

882   Manouze, H., Bouchatta, O., Gadhi, A.C., Bennis, M., Sokar, Z., Ba-M'hamed, S., 2017. Anti-inflammatory,

883   antinociceptive, and antioxidant activities of methanol and aqueous extracts of Anacyclus pyrethrum

884   roots. Front. Pharmacol. 8, 592-598.

885   Masresha, B., Makonnen, E., Debella, A., 2012. In vivo anti-inflammatory activities of Ocimum suave in

886   mice. J. Ethnopharmacol. 142, 201-205.

887   Mayer, D.J., Mao, J., Price, D.D., 1995. The development of morphine tolerance and dependence is

888   associated with translocation of protein kinase C. Pain 61, 365-374.

889   Mazzanti, G., Braghiroli, L., 1994. Analgesic antiinflammatory action of Pfaffia paniculata (Martius) kuntze.

890   Phytother Res 8, 413-416.

891   McCarson, K.E., Enna, S., 2014. GABA pharmacology: the search for analgesics. Neurochem. Res. 39, 1948-

892   1963.

893   Mequanint, W., Makonnen, E., Urga, K., 2011. In vivo anti-inflammatory activities of leaf extracts of

894   Ocimum lamiifolium in mice model. J. Ethnopharmacol. 134, 32-36.

895   Miller III, B.R., McGee Jr, T.D., Swails, J.M., Homeyer, N., Gohlke, H., Roitberg, A.E., 2012. MMPBSA. py: an

896   efficient program for end-state free energy calculations. J. Chem. Theory. Comput. 8, 3314-3321.

897   Ming-Tatt, L., Khalivulla, S.I., Akhtar, M.N., Lajis, N., Perimal, E.K., Akira, A., Ali, D.I., Sulaiman, M.R., 2013.

898   Anti-Hyperalgesic effect of a benzilidine-cyclohexanone analogue on a mouse model of chronic

899   constriction injury-induced neuropathic pain: Participation of the κ-Opioid receptor and KATP. Pharmacol.

900   Biochem. Behav. 114, 58-63.

901 Ming-Tatt, L., Khalivulla, S.I., Akhtar, M.N., Mohamad, A.S., Perimal, E.K., Khalid, M.H., Akira, A., Lajis, N.,

902 Israf, D.A., Sulaiman, M.R., 2012. Antinociceptive Activity of a Synthetic Curcuminoid Analogue, 2, 6-bis-

903 (4-hydroxy-3-methoxybenzylidene) cyclohexanone, on Nociception-induced Models in Mice. Basic Clin.

904 Pharmacol. Toxicol. 110, 275-282.

905 Monga, V., Goyal, K., Steindel, M., Malhotra, M., Rajani, D.P., Rajani, S.D., 2014. Synthesis and evaluation

906 of new chalcones, derived pyrazoline and cyclohexenone derivatives as potent antimicrobial,

907 antitubercular and antileishmanial agents. Med. Chem. Res. 23, 2019-2032.

908 Mousavi, S.R., 2016. Claisen–Schmidt condensation: Synthesis of (1S, 6R)/(1R, 6S)-2-oxo-N, 4, 6-

909 triarylcyclohex-3-enecarboxamide derivatives with different substituents in H2O/EtOH. Chirality 28, 728-

910 736.

911 Muhammad, N., Saeed, M., Khan, H., 2012. Antipyretic, analgesic and anti-inflammatory activity of Viola

912 betonicifolia whole plant. BMC. Complement. Altern. Med. 12, 53-59.

913 Nazar, M.F., Abdullah, M.I., Badshah, A., Mahmood, A., Rana, U.A., Khan, S.U.-D., 2015. Synthesis,

914 structure–activity relationship and molecular docking of cyclohexenone based analogous as potent non-

915 nucleoside reverse-transcriptase inhibitors. J. Mol. Struct. 1086, 8-16.

916 Okoth, D.A., Akala, H.M., Johnson, J.D., Koorbanally, N.A., 2016. Alkyl phenols, alkenyl cyclohexenones

917 and other phytochemical constituents from Lannea rivae (chiov) Sacleux (Anacardiaceae) and their

918 bioactivity. Med. Chem. Res. 25, 690-703.

919 Okoth, D.A., Koorbanally, N.A., 2015. Cardanols, long chain cyclohexenones and cyclohexenols from

920 Lannea schimperi (Anacardiaceae). Nat. Prod. Commun. 10, 103-106.

921 Olonode, E.T., Aderibigbe, A.O., Bakre, A.G., 2015. Anti-nociceptive activity of the crude extract of

922 Myrianthus arboreus P. Beauv (Cecropiaceae) in mice. J Ethnopharmacol 171, 94-98.

923   Patel, S., Naeem, S., Kesingland, A., Froestl, W., Capogna, M., Urban, L., Fox, A., 2001. The effects of GABAB

924   agonists and gabapentin on mechanical hyperalgesia in models of neuropathic and inflammatory pain in

925   the rat. Pain 90, 217-226.

926   Pini, L.A., Vitale, G., Ottani, A., Sandrini, M., 1997. Naloxone-reversible antinociception by paracetamol in

927   the rat. J. Pharmacol. Exp. Ther. 280, 934-940.

928   Rashid, U., Sultana, R., Shaheen, N., Hassan, S.F., Yaqoob, F., Ahmad, M.J., Iftikhar, F., Sultana, N., Asghar,

929   S., Yasinzai, M., 2016. Structure based medicinal chemistry-driven strategy to design substituted

930   dihydropyrimidines as potential antileishmanial agents. Eur. J. Med. Chem. 115, 230-244.

931   Rodrigues, M.R.A., Kanazawa, L.K.S., das Neves, T.L.M., da Silva, C.F., Horst, H., Pizzolatti, M.G., Santos,

932   A.R.S., Baggio, C.H., de Paula Werner, M.F., 2012. Antinociceptive and anti-inflammatory potential of

933   extract and isolated compounds from the leaves of Salvia officinalis in mice. J. Ethnopharmacol. 139, 519-

934   526.

935   Rukh, L., Ali, G., Ullah, R., Islam, N.U., Shahid, M.J.E.J.o.P., 2020. Efficacy assessment of salicylidene

936   salicylhydrazide in chemotherapy associated peripheral neuropathy. Eur. J. Pharmacol. 888, 173481.

937   Said, S.A., Amr, A.E.-G.E., Sabry, N.M., Abdalla, M.M., 2009. Analgesic, anticonvulsant and anti-

938   inflammatory activities of some synthesized benzodiazipine, triazolopyrimidine and bis-imide derivatives.

939   Eur. J. Med. Chem. 44, 4787-4792.

940   Salinas-Abarca, A.B., Avila-Rojas, S.H., Barragán-Iglesias, P., Pineda-Farias, J.B., Granados-Soto, V.J.E.j.o.p.,

941   2017. Formalin injection produces long-lasting hypersensitivity with characteristics of neuropathic pain.

942   Eur. J. Pharmacol. 797, 83-93.

943   Saranya, A.V., Ravi, S., 2012. Synthesis, Characterization and Anti-bacterial activity of pyrimidine,

944   cyclohexenone and 1, 5-diketone derivatives of Furfural Chalcone. J. Pharm. Res. 5, 1098-1101.

945   Sawynok, J., 1984. GABAergic mechanisms in antinociception. Prog. Neuropsychopharmacol. Biol.

946   Psychiatry. 8, 581-586.

947   Senguttuvan, S., Nagarajan, S., 2010. Synthesis of 2-amino-5-aryl-5, 6-dihydro-7-(naphthalen-2-yl)

948   quinazolin-4-ols. Int. J. Chem. 2, 108.

949   Sewell, R., Spencer, P., 1976. Antinociceptive activity of narcotic agonist and partial agonist analgesics and

950   other agents in the tail-immersion test in mice and rats. Neuropharmacology. 15, 683-688.

951   Shahid, M., Subhan, F., Ahmad, N., Ali, G., Akbar, S., Fawad, K., Sewell, R., 2017a. Topical gabapentin gel

952   alleviates allodynia and hyperalgesia in the chronic sciatic nerve constriction injury neuropathic pain

953   model. Eur. J. Pain. 21, 668-680.

954   Shahid, M., Subhan, F., Ahmad, N., Ullah, I., 2017b. A bacosides containing Bacopa monnieri extract

955   alleviates allodynia and hyperalgesia in the chronic constriction injury model of neuropathic pain in rats.

956   BMC. Complement. Altern. Med. 17, 293.

957   Shahid, M., Subhan, F., Ullah, I., Ali, G., Alam, J., Shah, R., 2016. Beneficial effects of Bacopa monnieri

958   extract on opioid induced toxicity. Heliyon 2, e00068.

959   Sheorey, R., Thangathiruppathy, A., Alagarsamy, V., 2016. Synthesis and Pharmacological Evaluation of 3-

960   propyl-2-substitutedamino-3H-quinazolin-4-ones as Analgesic and Anti-Inflammatory Agents. J.

961   Heterocycl. Chem. 53, 1371-1377.

962   Silva, R.H., Lima, N.d.F.M., Lopes, A.J., Vasconcelos, C.C., de Mesquita, J.W., de Mesquita, L.S., Lima, F.C.,

963   Ribeiro, M.N.d.S., Ramos, R.M., Cartágenes, M.d.S.d.S., 2017. Antinociceptive Activity of Borreria

964   verticillata: In vivo and In silico Studies. Front. Pharmacol. 8, 283.

965   Skidmore, I., Whitehouse, M., 1967. Biochemical properties of anti-inflammatory drugs—X: The inhibition

966   of serotonin formation in vitro and inhibition of the esterase activity of α-chymyotrypsin. Biochem.

967   Pharmacol. 16, 737-751.

968   Suba, V., Murugesan, T., Kumaravelrajan, R., Mandal, S.C., Saha, B., 2005. Antiinflammatory, analgesic and

969   antiperoxidative efficacy of Barleria lupulina Lindl. extract. Phytother. Res. 19, 695-699.

970   Systemes, D., 2015. BIOVIA, Discovery Studio Modeling Environment. Release 4.5. Dassault Systemes: San

971   Diego, CA.

972   Tjølsen, A., Berge, O.-G., Hunskaar, S., Rosland, J.H., Hole, K., 1992. The formalin test: an evaluation of the

973   method. Pain 51, 5-17.

974   Ullah, R., Ali, G., Subhan, F., Naveed, M., Khan, A., Khan, J., Halim, S.A., Ahmad, N., Al-Harrasi, A., 2021.

975   Attenuation of nociceptive and paclitaxel-induced neuropathic pain by targeting inflammatory, CGRP and

976   substance P signaling using 3-Hydroxyflavone. Neurochem. Int. 144, 104981.

977   Utsunomiya, I., Ito, M., Oh-ishi, S., 1998. Generation of inflammatory cytokines in zymosan-induced

978   pleurisy in rats: TNF induces IL-6 and cytokine-induced neutrophil chemoattractant (CINC) in vivo.

979   Cytokine 10, 956-963.

980   Van Hecke, O., Austin, S.K., Khan, R.A., Smith, B., Torrance, N., 2014. Neuropathic pain in the general

981   population: a systematic review of epidemiological studies. Pain 155, 654-662.

982   Wang, Y., Yu, C., Pan, Y., Li, J., Zhang, Y., Ye, F., Yang, S., Zhang, H., Li, X., Liang, G., 2011. A novel compound

983   C12 inhibits inflammatory cytokine production and protects from inflammatory injury in vivo. PLoS ONE

984   6, e24377.

985   Wisastra, R., Kok, P.A., Eleftheriadis, N., Baumgartner, M.P., Camacho, C.J., Haisma, H.J., Dekker, F.J., 2013.

986   Discovery of a novel activator of 5-lipoxygenase from an anacardic acid derived compound collection.

987   Bioorg. Med. Chem. 21, 7763-7778.

988   Yaouba, S., Koch, A., Guantai, E.M., Derese, S., Irungu, B., Heydenreich, M., Yenesew, A., 2018. Alkenyl

989   cyclohexanone derivatives from Lannea rivae and Lannea schweinfurthii. Phytochem. Lett. 23, 141-148.

990   Zanini Jr, J.C., Medeiros, Y.S., Cruz, A.B., Yunes, R.R., Calixto, J.B., 1992. Action of compounds from

991   Mandevilla velutina on croton oil-induced ear oedema in mice. A comparative study with steroidal and

992   nonsteroidal antiinflammatory drugs. Phytother. Res. 6, 1-5.

993 Maione, F., Colucci, M., Raucci, F., Mangano, G., Marzoli, F., Mascolo, N., Crocetti, L., Giovannoni, M.P., Di

994 Giannuario, A., Pieretti, S., 2020. New insights on the arylpiperazinylalkyl pyridazinone ET1 as potent

995 antinociceptive and anti-inflammatory agent. Eur. J. Pharmacol., 173572.

996

997

998

999

1000 **<u>FIGURE LEGENDS:</u>**

1001 **Fig. 1.** Chemical structure of Ethyl 6-(-4-methoxyphenyl)-2-oxo-4-phenylcyclohex-3-
1002 enecarboxylate

1003 **Fig. 2.** Agarose gel electrophoresis (A) quantification of CHD activity on the mRNA level of
1004 COX-2 **(B)**, TNF-α **(C),** and IL-1β **(D)** in carrageenan induced hind paw edema in mice. The results
1005 are shown in relative arbitrary units (A.U). Bars represent mean expression in A.U ± S.E.M. ###
1006 $P < 0.001$ compared to the saline group. **$P < 0.01$, ***$P < 0.001$ compared to the vehicle group.

1007 **Fig. 3.** Anti-nociceptive activity of (A) CHD and (B**)** the positive control, aspirin in the acetic acid
1008 (1%) induced abdominal constriction test. Each bar represents mean percentage protection ±
1009 S.E.M). *$P < 0.05$, **$P < 0.01$, ***$P < 0.001$ as compared to the saline treated group (one-way
1010 ANOVA followed by *post hoc* Dunnett's test), ($n = 6$ mice per group).

1011 **Fig. 4.** Anti-nociceptive activity of CHD and the positive control, tramadol, in the hot-plate test.
1012 Each bar represents mean percentage protection ± S.E.M). *$P < 0.05$, **$P < 0.01$, ***$P < 0.001$ as
1013 compared to saline treated group (one-way ANOVA followed by *post hoc* Dunnett's test), ($n = 6$
1014 mice per group).

Fig. 5. Anti-nociceptive activity of CHD and the positive control, tramadol in the thermal tail immersion test. Each bar represents mean withdrawal latency time in s ± S.E.M). *$P < 0.05$, **$P < 0.01$, ***$P < 0.001$ as compared to saline treated group (one-way ANOVA followed by *post hoc* Dunnett's test), ($n = 6$ mice per group).

Fig. 6. Anti-nociceptive activity of CHD and the positive controls, indomethacin (Indo), and diclofenac (Diclo) in the formalin induced paw nociceptive test. Each bar represents mean nociceptive response in s ± S.E.M). *$P < 0.05$, **$P < 0.01$, ***$P < 0.001$ as compared to the saline treated group (one-way ANOVA followed by *post hoc* Dunnett's test), ($n = 6$ mice per group).

Fig. 7. (A) Effect of naloxone at 1 mg/kg (NLX-1) and (B) PTZ at 15 mg/kg (PTZ-15) on the anti-nociceptive activity of CHD (30 mg/kg, CHD-30 and 45 mg/kg, CHD-45) or tramadol (30 mg/kg, TRD-30) in the mouse hot-plate test. Each bar represents mean percentage protection ± S.E.M. ***$P < 0.001$ compared to saline control (SAL). (two sample *t*-test), ($n = 6$ mice per group).

Fig. 8. Anti-inflammatory activity of (A) CHD and (B) the positive control, aspirin in the carrageenan induced paw edema test. Each bar represents paw volume in ml ± S.E.M. *$P < 0.05$, **$P < 0.01$, ***$P < 0.001$ as compared to saline treated group (one-way ANOVA followed by *post hoc* Dunnett's test), ($n = 6$ mice per group).

Fig. 9. Anti-inflammatory activity of (A) CHD and (B) the positive control, aspirin in the histamine induced paw edema test. Each bar represents paw volume in ml ± S.E.M. *$P < 0.05$, **$P < 0.01$, ***$P < 0.001$ as compared to saline treated group (one-way ANOVA followed by *post hoc* Dunnett's test), ($n = 6$ mice per group).

Fig. 10. Anti-inflammatory activity of (A) CHD and (B) the positive control, aspirin in the serotonin induced paw edema test. Each bar represents paw volume in ml ± S.E.M. *$P < 0.05$, **$P < 0.01$, ***$P < 0.001$ as compared to saline treated group (one-way ANOVA followed by *post hoc* Dunnett's test), ($n = 6$ mice per group).

Fig. 11. Anti-inflammatory activity of CHD and the positive controls, indomethacin (Indo), and diclofenac (Diclo) in the xylene induced ear edema test. Each bar represents ear weight in mg ± S.E.M. ***P**< 0.05, ****P**< 0.01, *****P**< 0.001 compared to the saline treated group (one-way ANOVA followed by *post hoc* Dunnett's test), (*n* = 6 mice per group).

Fig. 12. (A) Ribbon diagram of overlaid binding orientation of CHD and native ligand into the binding site of the COX-2 enzyme. **(B)** Three-dimensional ligand-enzyme interaction plots of the cyclohexenone derivative (CHD) into the binding site of COX-2 enzyme

Fig. 13. (**A**) Three-dimensional superimposed binding pose of the native ligand benzamidine (yellow), cyclohexenone derivative (CHD; purple) and methaqualone (orange) into the binding site of the GABA$_A$ receptor (PDB code 4COF) and (**B**) Two-dimensional interaction plot for CHD.

Fig. 14. Three and Two dimensional models of CHD binding with opioid receptors. (**A**) Three-dimensional and (**B**) Two-dimensional modeled superimposed binding pose of native ligand and CHD (purple) into the binding site of δ-opioid receptors (PDB code = 4EJ4). (**C**) Three-dimensional and (**D**) Two-dimensional model superimposed binding pose of native ligand and CHD (purple) into the binding site of κ-opioid receptor (PDB code = 4DJH). (**E**) Three-dimensional and (**F**) Two-dimensional model superimposed binding pose of the native ligand and selected compound CHD (purple) into the binding site of μ-opioid receptors (4DKL).

Fig. 15. (**A**) Root Mean Square Devitaions of backbone atoms for each receptor of docked complexes. (**B**) CHD Root Mean Square Devitaions over 50-ns of MD simulation in complex with receptors.